Synthesis of Ligand Targeted MRI Contrast Agent and Nanoparticles as Theranostic Tool for Hypoxic Solid Tumors

M.Sc. Thesis

by

Chetan Sharma

DISCIPLINE OF CHEMISTRY

INDIAN INSTITUTE OF TECHNOLOGY INDORE

JUNE 2019

Synthesis of Ligand Targeted MRI Contrast Agent and Nanoparticles as Theranostic Tool for Hypoxic Solid Tumors

A THESIS

Submitted in partial fulfillment of the requirements for the award of the degree of

Master of Science

by

Chetan Sharma

DISCIPLINE OF CHEMISTRY

INDIAN INSTITUTE OF TECHNOLOGY INDORE

JUNE 2019

INDIAN INSTITUTE OF TECHNOLOGY INDORE

CANDIDATE'S DECLARATION

I hereby certify that the work which is being presented in the thesis entitled **Synthesis of Ligand Targeted MRI Contrast Agent and Nanoparticles as Theranostic Tool for Hypoxic Solid Tumors** in the partial fulfillment of the requirements for the award of the degree of **MASTER OF SCIENCE** and submitted in the **DISCIPLINE OF CHEMISTRY, Indian Institute of Technology Indore**, is an authentic record of my own work carried out during the period from July 2018 to June 2019 under the supervision of **Dr. Venkatesh Chelvam**, Associate Professor, IIT Indore.

The matter presented in this thesis has not been submitted by me for the award of any other degree of this or any other institute.

Chetan Sharma

This is to certify that the above statement made by the candidate is correct to the best of my/our knowledge.

Dr. Venkatesh Chelvam

Chetan Sharma has successfully given his M.Sc. Oral Examination held on **July 01, 2019**

Signature of Supervisor of M.Sc. thesis
Date:

Convener, DPGC
Date:

Signature of PSPC Member
Dr. Sanjay Kumar Singh
Date:

Signature of PSPC Member
Dr. Anjan Chakraborty
Date:

ACKNOWLEDGEMENTS

With great pleasure, I want to express my deep sense of gratitude to my supervisor **Dr. Venkatesh Chelvam**, for the wonderful opportunity to pursue research and believing in my research abilities. His constant guidance, support, and motivation has been immensely helpful to complete this M.Sc. project. His enthusiasm and dedication has always inspired me.

Secondly I would also like express my deep sense of gratitude to my German host supervisor **Prof. Dr. Andreas Kirschning** and **Dr. Gerald Dräger** for giving me the golden opportunity to continue my master's thesis work in Leibniz Universitat Hannover, Germany from September 2018 to March 2019. His constant guidance, continuous support, encouragemnt, polite behaviour, and motivation has been immensely helped me to complete my project in given frame of time. I would also like to thanks DAAD master sandwich programme for the scholarship, accomodation, support etc.

Further, I would like to thank my PSPC members Dr. Sanjay Kumar Singh and Dr. Anjan Chakraborty for their valuable suggestions and support.

With great pleasure, I express my respect to Prof. Pradeep Mathur (Director, Indian Institute of technology Indore) for his unending encouragement and providing all the facilities at Indian Institute of Technology Indore.

I am grateful to Dr. Amrendra Kumar Singh (Head, Discipline of Chemistry) for his suggestions and guidance in various aspects. I am also grateful to Dr. Tridib Kumar Sarma, Dr. Suman Mukhopadhyay, Dr. Apurba Kumar Das, Dr. Sampak Samantha, Dr. Biswarup Pathak, Dr. Tushar Kanti Mukherjee, Dr. Rajneesh Misra and Dr. Satya S. Bulusu for their guidance and help during various activities.

I would like to extend my deep and sincere thanks to Sagnik Sengupta, Ramesh B. Reddy, A V R Krishna Rao, Maik, Christian, Tim, Janein, Sibel, Göran, Teresa, Friederike, Alexey, Samhita, Siebel, Li, Helge Berneaud and Dr. Mathew Norris for their guidance, encouragement, and support.

I extend my deep thanks to my group members Amit Pandit, Premansh Dudhe, Srija Tiwari, Aishi and Mena Asha Krishnan for their selfless co–operation and help to make my work successful.

I would also like to thank technical staff from Sophisticated Instrumentation Center (SIC), IIT Indore, Ms. Sarita Batra, Mr. Kinny Pandey, Mr. Ghanshyam Bhavsar and Mr. Manish Kushwaha for their patience and timely technical support without which it was impossible to continue with my work. I would also like to thank Ms. Anjali Bandiwadekar, Mr. Rajesh Kumar, Mr. Lala Ram Ahirwar and other library staff.

I personally want to extend my thanks to my friend Vivek Chauhan and my all batch mates who were always there and never let me down during these M.Sc. days. Most importantly none of this would have been possible without the support of my family. I deeply express my love and gratitude to my father Sh. Ram Dutt Sharma and my mother Mrs. Radha Devi. I want to extend my deep love and thanks to my sisters Sonu Upadhyay, Manju, Anjali and my brothers Hari Om and SRK Pasi.

Finally, I would like to express my thanks to IIT Indore and Leibniz Universität Hannover Germany for infrastructure and all others who helped and supported me directly or indirectly.

Chetan Sharma

DEDICATION

This thesis is dedicated to my family……

Abstract

Carbonic anhydrase (CA) is a Zinc metalloenzyme which catalyzes the interconversion of carbon dioxide into proton and bicarbonate. Most of the human cancers overexpresses CA IX which helps to control the hypoxic microenvironment in the cells. In this work, we have synthesized a ligand targeted MRI contrast agent for diagnosis of aggressive tumor progression and a ligand targeted therapeutic tool to deliver iron oxide nanoparticles.

Iron oxide nanoparticles are being actively investigated to achieve highly efficient carcinogenic cell destruction through magnetic hyperthermia treatments . The designed molecule consists of three components: a) a small molecule inhibitor specific to the protein of interest e.g. aromatic sulphonamide derivative b) a peptidic spacer to enhance the distance between targeting ligand and the attached nanoparticle so, that the specific binding affinity of the ligand to the protein is not compromised and c) functionalized deliverable nanoparticle (Fe_3O_4) for MRI contrast agent as well as for magnetic hyperthermia treatment.

TABLE OF CONTENTS

LIST OF FIGURES

LIST OF SCHEMES

LIST OF TABLES

SYMBOLS/UNITS

λ	Wavelength
δ	Chemical shift
nm	Nanometer
°C	Degree Celsius
mmol	Millimole
M	Molar
g	Gram
h	Hour
J	Coupling constant
nM	Nano molar
mL	Milli litre
dd	Doublet of doublet
Hz/MHz	Hertz/Mega Hertz
R_f	Retention factor
ppm	Parts per million

ACRONYMS

TMS	Tetramethylsilane
NMR	Nuclear Magnetic Resonance
DCM	Dichloromethane
ACN	Acetonitrile
HRMS	High Resolution Mass Spectroscopy
$CHCl_3$	Chloroform
CH_3	Methyl
$CDCl_3$	Chloroform-d
Et_3N	Triethylamine
THF	Tetrahydrofuran
DMF	*N*,*N*-Dimethyl formamide
APTES	3-Aminopropyltriethoxysilane
Na_2SO_4	Sodium sulphate
OH	Hydroxyl
HATU	1-[Bis(dimethylamino)methylene]-1*H*-1,2,3-triazolo[4,5-b]pyridinium 3-oxidhexafluorophosphate hexafluorophosphateazabenzotriazole tetramethyl uronium
DIPEA	*N*,*N*-Diisopropylethylamine
TFA	Triflouroacetic acid
TIS	Triisopropylsilane
EDT	1,2-Ethanedithiol
NHS	*N*-Hydroxysuccinimide
DCC	*N*,*N*-dicyclohexylcarbodiimide
MPA	Mercaptopropionic acid
NPs	Nanoparticles
CA	Carbonic anhydrase
DMSO	Dimethyl sulfoxide

PEG	Polyethylene glycol
IONP	Iron oxide nanoparticles
s	Singlet
d	Doublet
dd	Doublet of doublet
t	Triplet
m	Multiplet

Chapter 1

Introduction

1.1. General Introduction

Hypoxia is a condition commonly present in the later stage of cancer when cancer cells begin to metastasize. At this stage, tumors cells are deprived of oxygen (typically ≤1% of overall oxygen content) due to its rapid proliferating nature and change in their metabolic activity [1]. This metabolic transition and rapid proliferation cause a decrease in extracellular pH (~6.5) in the microenvironment of the tumor cells due to the formation of excess lactic acid [1–2]. This hypoxic stress alters so many factors such as cell proliferation, angiogenesis, cell motility, invasiveness, and often resistance to common anti-cancer treatments. As a result, it creates a hindrance in the treatment of aggressive cancers. Since 1930, it has been well established that there is a relation between tumor hypoxia and resistance to chemotherapy [3–4]. Hypoxic tumors became resistant to common chemotherapeutics and have a high tendency to metastasize. Hence, tumor hypoxia is a lethal pathological diseased condition and associated with poor patient prognosis [4]. To survive in this acidic microenvironment, tumor cells must adjust an intracellular pH at physiological levels (pH 7.4) [6]. Therefore, carbonic anhydrase (CA), a family of zinc metalloenzymes plays an important role in this regulatory process. The CA catalyzes the reversible hydration of carbon dioxide to form bicarbonate and a proton [7]. Humans express fifteen carbonic anhydrase isoforms and of these, CA IX and CA XII have been shown to be associated with hypoxic tumors. Both these enzymes are transmembrane proteins with an extracellular catalytic domain and upregulated in solid tumors while exhibiting low expression in normal tissues (CA IX expression only) [8]. Among these two metalloenzymes, CA IX has been shown to be more prevalent in solid tumors compared to CA XII. Therefore, CA IX has been identified as a promising therapeutic target to treat hypoxic tumors [7–9,10]. Recently, Low et al described

delivery of cytotoxic molecule by conjugating with a small molecule inhibitor specific for CA IX receptor [11]. Therefore, CA IX is an important biomarker for the treatment of hypoxic solid tumors.

We have been working on targeted drug delivery techniques to detect and treat various cancers [12–15] and inflammatory diseases [16–18] using small molecule targeting ligands. Many of these techniques are USA patented and at present in various stages of preclinical and clinical development for treating cancer patients [19–21].

Paramagnetic iron oxide nanoparticles could also be used for diagnosis as an MRI contrast agent. However, iron oxide nanoparticles are generally used as negative contrast agents (T_2-weighted images) which produce signal decreasing effect. The resulting signal could be interpreted wrongly with the other pathological conditions. Moreover, T_2 contrast agents distort magnetic field in the neighboring healthy tissues resulting in dark images with no background around the lesions. Whereas T_1 contrast agents such as high-spin paramagnetic Gd^{3+} ions produce hyperintense signals in T_1-weighted images. Several Gd^{3+} contrast agents have been approved by the European Medical Agency (EMEA) and the US Food and Drug Administration to provide better images of organs and tissues.

1.2. Aim of the project

In continuation of our interest, our aim in this project is to develop a ligand-targeted Magnetic Resonance Imaging (MRI) contrast agent for diagnosis of aggressive tumor progression followed by treatment with ligand-targeted releasable iron oxide (Fe_3O_4) nanoparticles [22]. The synthesized ligand selectively targets the carbonic anhydrase (CA IX) receptor, which is overexpressed in most of the hypoxic solid tumors. The proposed multimodal tool consists of three components i) a small molecule ligand (e.g. aromatic sulphonamide derivative) specific to the protein of interest (CA IX), which is overexpressed in diseased condition ii) a peptidic spacer to enhance the distance between targeting ligand and the attached cargo so that the specific binding affinity of the ligand to the protein is not compromised and iii) MRI contrast agent for diagnosis and functionalized releasable iron oxide

nanoparticles for treatment of hypoxic solid tumors through magnetic hyperthermia treatment [23–25].

Chapter 2

Literature

In 1954, acetazolamide was the first reported carbonic anhydrase inhibitor [29] for the treatment of glaucoma, altitude sickness, convulsant, epilepsy, periodic paralysis, etc. To date approximately, 25 drugs are used to treat diseases like glaucoma, convulsions, high-altitude sickness and cancer [30]. Many of these drugs have side effects, because they inhibit different isoforms of carbonic anhydrase, which are not involved in the targeted disease. Therefore, this area remains unexplored and there is an urgency to develop inhibitors that are selective to various CA enzymes [30]. This motivated researchers to synthesize small molecules which will selectively bind with the desired CA isoform. Aromatic and heterocyclic sulfonamides are the best class of carbonic anhydrase inhibitors [31]. The binding affinity of the aromatic sulfonamide highly depends on the pKa of the sulfonamide group which is ~11.0. For the better binding, the pKa value should be near 7.4 [32, 33]. Presence of electronegative group decreases the pKa of aromatic sulfonamide and enhances the carbonic anhydrase inhibitory properties. Thus, fluorinated benzene sulfonamide can be used as carbonic anhydrase inhibitors. In the past few years, several research groups synthesized different polyfluorinated and non-fluorinated sulfonamide derivatives and analyzed their inhibitory properties against different isoforms of carbonic anhydrase. Later these CA small molecule inhibitors have been used for the delivery of cytotoxic drugs to the diseased tissue. Cazzamalli et *al*. [27] and Krall et *al*. [28] have utilized acetazolamide [FDA approved] CA IX inhibitor as a small molecule targeting ligand for the delivery of cytotoxic drug like monomethyl auristatin E, duocarmycin, and maytansine to treat solid hypoxic tumors. Recently Low et *al*. have developed a small molecule CA IX targeted tubulysin B conjugate to kill CA IX expressing tumors [11].

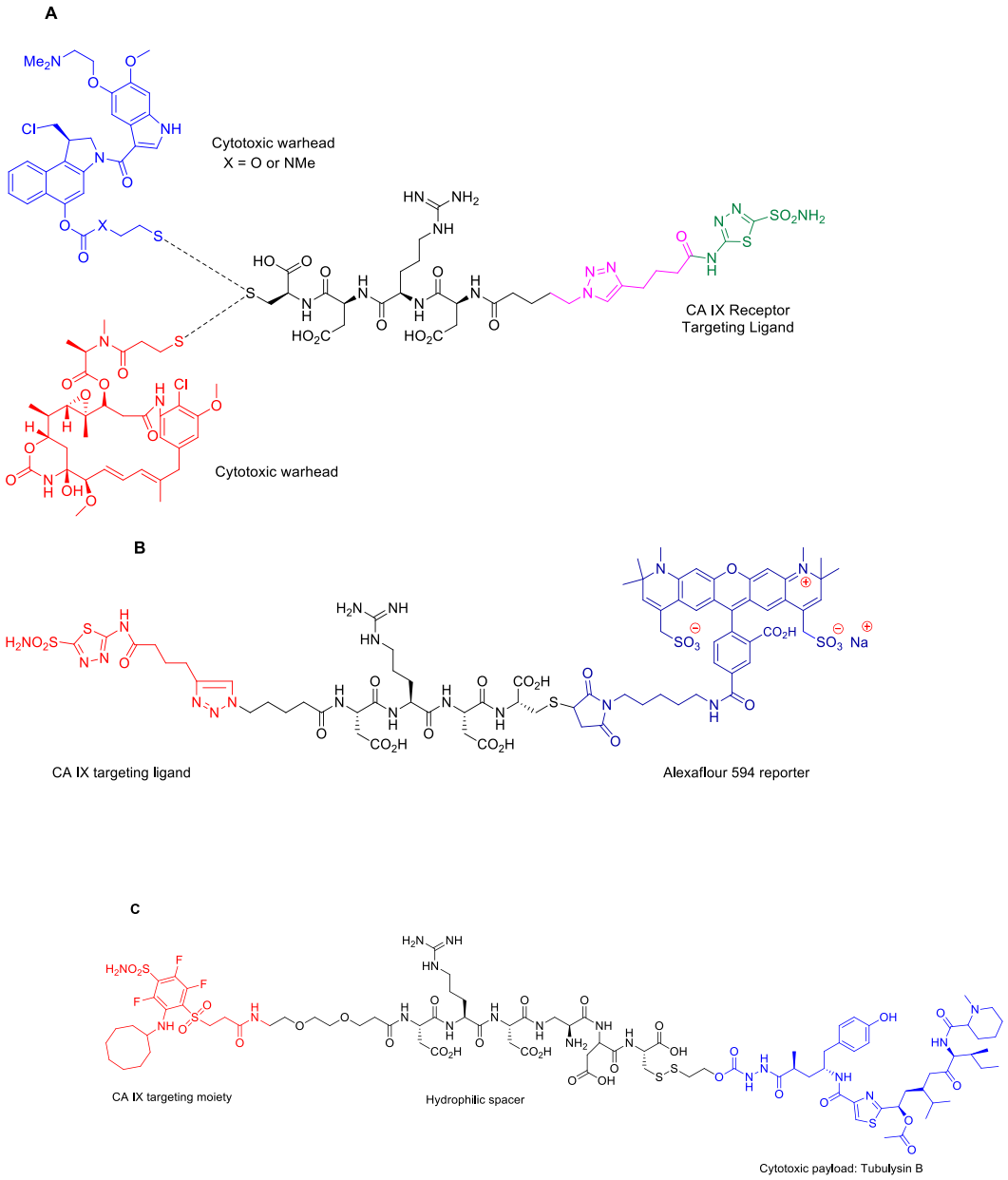

Figure 1. (**A**) Small molecule ligand targeted drug conjugates (**B**) CA IX targeted alexa flour 594 conjugate (**C**) CA IX targeted tubulysin B conjugate

Chapter 3

Experimental Section

3.1. Materials and methods

Analytical grade *N*,*N*–dimethylformamide (DMF) for solid phase synthesis was bought from TCI chemicals. All other solvents or reagents were used as such as supplied by Fisher chemicals, Merck and Sigma Aldrich. 1,2-Diaminoethane trityl and H-Cys(Trt)-2-chlorotrityl resins were purchased from Iris biotech. All the reactions were performed in oven-dried glasswares under an inert atmosphere with magnetic stirring. Air and moisture sensitive liquids and solutions were transferred by using glass syringes under nitrogen atmosphere. All reagents were obtained from commercial sources and used as such unless otherwise stated. Solvents were distilled using suitable drying agents (CaH_2 or Na wire, Mg turnings) under nitrogen atmosphere. Reactions were monitored by thin layer chromatography using Merck silica gel 60 F254 TLC glass plates. Evaporation of volatile solvents were carried out under reduced pressure using rotary evaporator at 40 °C and appropriate reduced pressure. ^{1}H, ^{19}F and ^{13}C NMR spectra were recorded using Bruker AV 400MHz NMR spectrometer with TMS as an internal reference. $CDCl_3$ and DMSO-d_6 were used as NMR solvents. Chemical shift is reported in delta (δ) units, expressed in parts per million (ppm) downfield from tetramethylsilane (TMS). The HR-MS spectra of the compounds were recorded by using Bruker Daltonics MicroTOF-Q II mass spectrometer using methanol as solvent. FT-IR spectra of samples dissolved in CH_2Cl_2 were recorded using Fourier Transform Infrared-Attenuated Total Reflection (FTIR-ATR) Spectrometer, Bruker (Tensor-27) over a range of 500–4000 cm^{-1}. High-Resolution Mass Spectrometry (HR-MS) spectra and analytical reversed-phase Ultra Performance Liquid Chromatography (UP-MS) were performed on a Waters xevo G2-XS QTOF coupled to a waters acquity UPLC H-class system with PDA UV detector, using a ACQUITY UPLC BEH C_{18} column, 130 Å, 1.7 µm, 2.1 mm × 50 mm at a flow rate of 0.6 ml min^{-1} with linear gradients of solvents A and B (A = Millipore water with 0.1% formic

acid, B = MeCN with 0.1% formic acid). The preparative reversed-phase high-pressure liquid chromatography (RP-HPLC) were performed on a Waters alliance HT RP-HPLC with PDA UV detector, using a Synergi 4µm, Polar-RP 80Å 10 × 150 mm C_{18} column at a flow rate of 4 ml min^{-1} with linear gradient of solvents A and B (A = HPLC grade water with 0.1% formic acid, B = Methanol with 0.1% formic acid).

3.2. Synthesis of pentaflourobenzene sulfonamide (2)

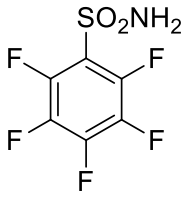

2

Pentaflourobenzenesulfonyl chloride **1** (2.90 g, 10.86 mmol) was dissolved in dry THF (130 mL) in a 250 mL round bottom flask. The reaction mixture was cooled to –10 °C and 30% aq. ammonia (3.46 mL, 86.95 mmol) was added dropwise to the reaction mixture with stirring. The progress of reaction was monitored by TLC. After the completion of reaction, THF was evaporated under reduced pressure using rotatory evaporator. The crude product was purified by chromatography on a column of silica gel (230–400 mesh) using 1.5:8.5 mixture of ethyl acetate in hexane to get the titled pentaflourobenzene sulfonamide **2 (**2.41 g, 90%) as a white solid. m.p. 155–157 °C. TLC: R_f 0.54 (2.5:7.5 EtOAc/hexane). IR: 3424, 3344 (N–H), 1641 (C=C) cm^{-1}. ^{1}H NMR (400 MHz, DMSO-d_6): δ 8.46 (s, 2H). ^{13}C NMR (100 MHz, DMSO-d_6): δ 145.0, 142.4, 139.1, 136.2, 119.5 ppm. ^{19}F NMR (400 MHz, DMSO-d_6): δ –139.04 (d, J = 22.6 Hz, 2F), –148.90 (t, J = 23.70 Hz, 1F), –160.5094 (t, J = 23.70 Hz, 2F).

3.3. Synthesis of 6-((2,3,5,6-tetrafluoro-4-sulfamoylphenyl)amino) hexanoic acid (4)

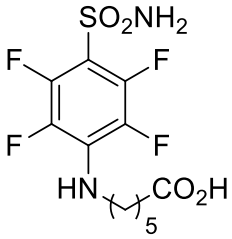

4

Pentaflourobenzene sulphonamide **2** (2.26 g, 9.16 mmol) was dissolved in DMSO (7 mL) in a round bottom flask (25 mL) and stirred at room temperature. 6-Aminohexanoic acid **3** (1.32 g, 10.08 mmol) and triethylamine (1.30 mL, 9.26 mmol) was added to the reaction mixture at room temperature. The reaction mixture was heated at 80 °C for 24 h. The progress of

reaction was monitored by TLC. After 24 h, the reaction mixture was cooled to ambient temperature and 4 mL of HPLC grade methanol was added to the reaction mixture. The crude product was purified by reversed-phase high-performance liquid chromatography (RP-HPLC) using C_{18} reverse-phase column to get the tilted product **4** (1.80 g, 62%) as viscous oil. [A = 0.1 % formic acid in HPLC grade water and B = 0.1% formic acid in HPLC grade methanol, solvent gradient: 5% B to 100% B in 80 min, 100 min, flow rate = 15 mL/min]. TLC: R_f 0.12–0.25 (6:4 EtOAc/hexane). m.p. 143–145 °C. IR: 3417.86, 3375.43, 3282.4 (–NH, $–NH_2$), 2941.44 (–OH), 2875.86 (C–H), 1697.36 (C=O), 1357.89–1388.75 (S=O) cm^{-1}. ^{1}H NMR (400 MHz, DMSO-d_6): δ 12.01 (s, 1H), 7.92 (s, 2H), 6.71 (s, 1H), 2.20 (t, J = 6.64 Hz, 2H), 1.44–1.59 (m, 5H), 1.17–1.36 (m, 3H) ppm. ^{13}C NMR (100 MHz, DMSO-d_6): δ 174.5, 144.9, 142.5, 136.8, 134.4, 131.3, 107.5, 44.0, 33.6, 30.0, 25.6, 24.2 ppm. ^{19}F NMR (100 MHz, DMSO-d_6): δ –161.20 (d, J = 18.04 Hz, 2F), –142.24 (d, J = 18.04 Hz, 2F) ppm. HRMS (ESI) m/z $[M+Na]^+$ calcd. for $C_{12}H_{14}F_4N_2O_4S$ 381.0508, found 381.0507.

3.4. Synthesis of 6-((3-(cyclooctylamine)-2,5,6-trifluoro-4-sulfamoylphenyl) amino) hexanoic acid (6)

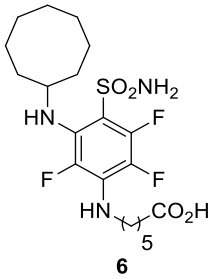

6

6-((2,3,5,6-Tetrafluorosulfamoylphenyl)amino) hexanoic acid **4** (1.678 g, 4.68 mmol) was dissolved in DMSO (4 mL) in a round bottom flask (10 mL) and stirred at room temperature. Cyclooctylamine **5** (1.28 mL, 9.37 mmol) and triethylamine (1.30 mL, 9.37 mmol) was added dropwise to the reaction mixture with stirring. The reaction mixture was heated at 70 °C for 24 h. The progress of reaction was monitored by TLC and LC-MS. After 24 h, the reaction mixture was cooled to ambient temperature and HPLC grade methanol (2 mL) was added to the reaction mixture. The crude product was purified by RP-HPLC by using C_{18} reverse phase column to get the tilted product **6** (697.17 mg, 32 %) as a viscous oil. [A = 0.1 % formic acid in HPLC grade water and B = 0.1% formic acid in HPLC grade methanol, solvent gradient: 5% B to 100% B in 80 min, 100 min, flow rate = 15 mL/min]. TLC: R_f 0.44–0.56. ^{1}H NMR (400 MHz, DMSO-d_6): δ 11.97 (brs, 1H), 7.65 (s, 2H), 6.14 (d, J = 9.12 Hz, 1H), 6.06 (brs, 1H), 3.57–

3.70 (m, 1H), 3.24–3.28 (m, 2H), 2.19 (t, J = 7.36 Hz, 2H), 1.74–1.84 (m, 2H), 1.60–1.68 (m, 2H), 1.41–1.55 (m, 14H), 1.23–1.32 (m, 2H) ppm. ^{13}C NMR (100 MHz, DMSO-d_6): δ 174.4, 145.1 (d, J = 8.79 Hz), 138.0 (d, J = 3.7 Hz), 136.3 (d, J = 4.17 Hz), 133.3 (dd, J = 11.57 Hz, 4.49 Hz), 131.8 (dd, J = 11.57 Hz, 4.49 Hz), 130.9, 105.9 , 55.0 (d, J = 7.07 Hz), 44.1, 33.6, 32.1, 30.0, 26.8, 25.6, 25.1, 24.2, 23.0 ppm. ^{19}F NMR (400 MHz, DMSO-d_6): δ –139.52 (dd, J = 25.08 Hz, 7.48 Hz, 1F), –149.17 (s, 1F), –169.20 (d, J = 25.08 Hz, 1F) ppm. HRMS (ESI) m/z $[M+H]^+$ calcd. for $C_{20}H_{30}F_3N_3O_4S$ 466.1987, found 466.1988.

3.5. Synthesis of N-(2-(2-(3-((2-aminoethyl) amino)-3-oxopropoxy) ethoxy) ethyl)-6-((3-(cyclooctylamino)-2,5,6-trifluoro-4-sulfamoylphenyl) amino)-hexanamide (11)

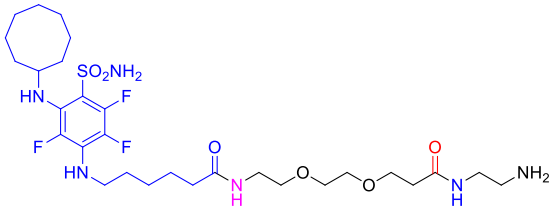

11

1,2-Diaminoethanetrityl resin **7** (100 mg, 0.58 g/mol) was swollen with DCM (3 mL) for 30 min by bubbling low stream of argon gas through resin beads in the peptide synthesis vessel (15 mL) which was attached to round bottom flask (250 mL). After 30 min, DCM was drained using suction pump followed by swelling the resin with DMF (3 mL) for 30 min by bubbling low stream of argon gas. A solution of Fmoc-AEEP **8** (46.33 mg, 0.12 mmol), HATU (62 mg, 0.16 mmol) and DIPEA (50 µL, 0.29 mmol) in DMF (3 mL) was added to the peptide vessel containing resin beads and the coupling reaction was continued for 3 h by bubbling low stream of argon gas. The resin beads were washed with DMF (3 × 3 mL) and then with isopropanol (3 × 3 mL). The resin beads were dried under reduced pressure for 5 min and the completion of coupling reaction was confirmed by the Kaiser test.

The Kaiser test reagents were prepared in three different glass bottles: 1) Dissolve 100 mg ninhydrin in 2 mL of ethanol 2) Dissolve 80 g phenol in 20 mL ethanol

3) Dilute 2 mL of a 0.001 M solution of KCN to 100 mL with pyridine

After preparing the Kaiser test kit, few dried resin beads were taken in a test tube (5 mL) and 2 drops, each of ninhydrin, phenol, and 0.1% potassium cyanide solution as described above, were added to the resin beads. The test tube was heated at 110 °C for 2 min on sand bath. Appearance of colorless beads indicates absence of free amino group and completion of coupling reaction. A freshly prepared solution of 20% piperidine in DMF (5 mL) was added to the resin beads in the peptide vessel and low stream argon gas was bubbled through the resin beads for 10 min. After 10 min, the deprotecting reagent was drained using suction pump. The deprotection step was repeated twice by addition of 5 mL 20% piperidine in DMF twice to ensure complete deprotection of NHFmoc. The resin beads were washed with DMF (3 × 3 mL) and then with isopropanol (3 × 3 mL). The formation of free amine group was confirmed by performing Kaiser test as described above. A solution containing ligand **6** (31 mg, 0.07 mmol), HATU (62 mg, 0.16 mmol) and DIPEA (50 μL, 0.29 mmol) in DMF (3 mL) was added to the resin beads using micro pipette and argon gas was bubbled for 3 h. The resin beads were washed with DMF (3 × 3 mL) and then with isopropanol (3 × 3 mL). The coupling reaction was confirmed by performing the Kaiser test. The functionalized resin beads were dried under reduced pressure for 10 min. 5 mL of freshly prepared TFA/TIS/EDT/H_2O cleavage cocktail (92.5:2.5:2.5:2.5) was added to the resin beads and low stream argon gas was bubbled for 40 min and the mother liquor was collected into a 25 mL round bottom flask. The cleavage reaction was repeated twice by addition of 2.5 mL of cleavage cocktail for 5 min to ensure complete cleavage of the ligand attached peptide conjugate from the resin beads. The cleavage cocktail was evaporated under reduced pressure using rotatory evaporator. The concentrated viscous liquid was precipitated in a 10 mL pear-shaped flask by addition of 5 mL of ice-cold diethyl ether. The pear-shaped flask was placed in an ice bath for 30 min. The ether layer from the pear-shaped flask was slowly decanted without disturbing the settled oily precipitate. The precipitate was washed twice with ice-cold diethyl (2 × 3 mL) ether to remove triflouroacetic acid and ethanedithiol residues completely. Diethyl ether was evaporated under reduced pressure using rotatory evaporator. The crude peptide conjugate was purified by RP-HPLC using

C_{18} reversed-phase column to obtain pure ligand attached peptide conjugate **11** (26.29 mg, 68 %) as a viscous oil. [A = 0.1 % formic acid in water and B = 0.1 % formic acid in HPLC grade methanol, solvent gradient: 5% B to 100% B in 80 min, 100 min, flow rate = 15 mL/min). Retention time = 48–52 min. ^{1}H NMR (400 MHz, DMSO-d_6): δ 8.38 (s, 2H), 8.30 (s, 1H), 7.87 (s, 1H), 6.39 (d, J = 9.72 Hz, 1H), 6.14 (d, J = 9.72 Hz, 1H), 6.06 (brs, 1H), 5.81 (s, 1H), 3.59 (t, J = 6.24 Hz , 3H), 3.37 (t, J = 5.88 Hz, 2H), 3.12–3.28 (m, 6H), 2.83 (s, 4H), 2.74 (t, J = 5.88 Hz, 2H), 2.32 (t, J = 6.24 Hz, 2H), 2.01–2.09 (m, 2H), 1.72–1.85 (m, 2H), 1.59–1.71 (m, 2H), 1.33–1.57 (m, 14H), 1.16–1.30 (m, 2H) ppm. ^{19}F NMR (400 MHz, DMSO-d_6): δ –140.98 (dd, J = 25.60 Hz, 7.76 Hz, 1F), –148.81 (s, 1F), –168.86 (d, J = 25.60 Hz, 1F) ppm. HRMS (ESI) m/z $[M+H]^+$ calcd. for $C_{29}H_{49}F_3N_6O_6S$ 667.3465, found 667.3465.

3.6. Synthesis of (3-(cyclooctylamino)-2,5,6-trifluoro-4-sulfamoylphenyl) amino)-2-(mercaptomethyl)-4,14-dioxo-7,10-dioxa-3,13-diazanonadecan-1-oic acid (16).

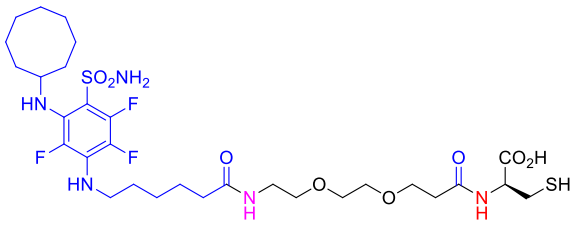

16

H-Cys(Trt)-2-chlorotrityl resin **12** (100 mg, 0.64 g/mol) was swollen with DCM (3 mL) for 30 min by bubbling low stream of argon gas through resin beads in the peptide synthesis vessel (15 mL) which was attached to the round bottom flask (250 mL). After 30 min, DCM was drained using a suction pump followed by swelling with DMF (5 mL) for 30 min with a low stream of argon gas. A solution of Fmoc-AEEP **8** (46.33 mg, 0.12 mmol), HATU (62 mg, 0.16 mmol) and DIPEA (50 µL, 0.29 mmol) in DMF (3 mL) was added to the peptide vessel containing resin beads and the coupling reaction was continued for 3 h by bubbling low stream of argon gas. The resin beads were washed with DMF (3 × 3 mL) followed by isopropanol (3 × 3 mL). The resin beads were dried under reduced pressure for 5 min and the completion of peptide coupling reaction was confirmed by performing the Kaiser test. A freshly prepared solution of 20% piperidine in DMF (5 mL) was added to

the resin beads in the peptide vessel and a low stream argon gas was bubbled through the beads for 10 min. After 10 min, the deprotection reagent was drained using suction pump. The procedure was repeated twice by addition of 5 mL of 20% piperidine in DMF to ensure complete deprotection of NHFmoc. The resin beads were washed again with DMF (3 x 3 mL) and then with isopropanol (3 × 3 mL). The formation of free amine group was confirmed by performing the Kaiser test. A solution of **6** (34.50 mg, 0.07 mmol), HATU (60.84 mg, 0.16 mmol) and DIPEA (56 μL, 0.32 mmol) in DMF (3 mL) was added to the peptide vessel containing swollen resins and a low stream argon gas was bubbled for 3 h. The resin beads were washed with DMF (3 × 3 mL) and then with isopropanol (3 × 3 mL). The coupling reaction was confirmed by performing the Kaiser test. The functionalized resin beads were dried under reduced pressure for 10 min. 5 mL of freshly prepared TFA/TIS/EDT/H_2O cleavage cocktail (95:2.5:2.5:2.5) was added to the resin beads and a low stream argon gas was bubbled for 40 min. The mother liquor was collected into a 25 mL round bottom flask. The cleavage reaction was repeated twice by addition of 2.5 mL of cleavage cocktail for 5 min to ensure complete cleavage of peptide chain from the resin beads. The cleavage cocktail was evaporated under reduced pressure using rotatory evaporator. The concentrated viscous oil was precipitated in a 10 mL pear-shaped flask by addition of 5 mL of ice-cold diethyl ether. The pear-shaped flask was cooled in an ice bath for 30 min. The ether layer was slowly decanted from the pear-shaped flask without disturbing the settled oily precipitate. The precipitate was washed twice with ice-cold diethyl ether (2 × 5 mL) to remove the traces triflouroacetic acid and ethanedithiol completely. Ether was evaporated under reduced pressure using rotatory evaporator. The crude conjugate product was purified by RP-HPLC using C_{18} reversed-phase column to get the titled product **16** (28.88 mg, 62%). as a viscous oil. [A = 2 mM ammonium acetate buffer (pH = 5.0) and B = acetonitrile, solvent gradient: 5% B to 100% B in 80 min, 100 min, flow rate = 15 mL/min, retention time = 36–40 min. HRMS (ESI) m/z $[M+Na]^+$ calcd. for $C_{30}H_{48}F_3N_5O_8S_2$ 728.2975, found 728.2961.

3.7. Synthesis of *N*-succinimidyl-3-(2-pyridyldithio)propionate (19)

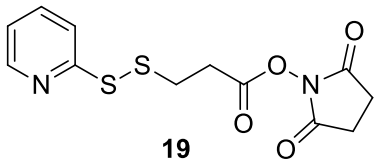

19

2-Aldrithiol **22** (2.00 g, 9.08 mmol) was dissolved in dry ethanol (40 mL) in a round bottom flask (100 mL) and stirred at room temperature. A solution of 3-mercaptopropanoic acid **23** (0.40 mL, 4.52 mmol) in dry ethanol (2 mL) and acetic acid (50 μL, 3.48 mmol) was added dropwise to the stirring reaction mixture. The reaction mixture was stirred for 4 h. The progress of reaction was monitored by TLC. After 4 h, the solvent was evaporated under reduced pressure to yield yellowish oil which was dried under reduced pressure for 2 h to remove the traces of acetic acid. The yellowish oily crude product was purified by chromatography on a basic alumina column using a 2:3 mixture of ethanol in DCM as eluent. After the elution of yellow band containing 2-mercaptopyridine from the column, 4 mL of AcOH was added in 100 mL of 2:3 mixture of ethanol in DCM to elute 3-(2-pyridyldithio)propanoic acid **24** in 70% purity.

Dry DCM was cooled to 0 ℃ in a two neck round bottom flask (50 mL). 3-(2-Pyridyldithio)propanoic acid **24** (500 mg, 2.32 mmol) was dissolved in cooled DCM (10 mL) at 0 ℃ under N_2 atmosphere. DCC (528 mg, 2.55 mmol) and NHS ester (295 mg, 2.55 mmol) was added to the reaction mixture and the reaction mixture was stirred for 10 min at 0 ℃. After 10 min, the reaction mixture was warmed to ambient temperature and stirred further for 3 h at room temperature. The progress of reaction was monitored by TLC. After the completion of reaction, the reaction mixture was filtered to remove precipitated urea and the filtrate was collected in a 50 mL round bottom flask. The solvent was evaporated under reduced pressure using rotatory evaporator to yield yellowish oily crude product **19**. The crude **19** was purified by chromatography on a column of silica gel (230–400 mesh) using 1:1 mixture of EtOAc in hexane to obtain **19** (507.27 mg, 70%) as a colourless oil and stored at –20 ℃ in a refrigerator. ^{1}H NMR (400 MHz, $CDCl_3$): δ 8.47–8.52 (m, 1H), 7.63–7.70 (m, 2H), 7.08–7.15 (m, 1H), 3.05–3.16 (m, 4H), 2.84 (s, 4H) ppm. ^{13}C NMR (100 MHz, $CDCl_3$): δ 169.0, 167.1, 159.3, 150.0, 137.4, 121.2, 120.1, 32.9, 31.1, 25.7 ppm.

3.8. General procedure for the synthesis of iron (III) oxide nanoparticles (17)

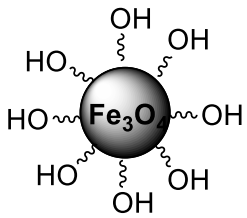

17

3.8.1. In a two-neck round bottom flask (250 mL), 100 mL of water was deoxygenated by bubbling N_2 gas for 40 min. Ferrous sulfate heptahydrate **25** (200 mg ,0.72 mmol) and ferric chloride hexahydrate **26** (232 mg, 1.44 mmol) were dissolved in 100 mL of deoxygenated water with vigorous stirring at room temperature. 2 mL of aq. ammonia (28–30%) was added dropwise to the reaction mixture and heated to 85 °C for 2 h. After 2 h, the reaction mixture was cooled to ambient temperature. The black precipitate was washed five times with distilled water (5 × 10 mL) and twice with ethanol (10 mL) followed by magnetic decantation. The precipitated particles were dried at 40 °C under reduced pressure for 24 h.

3.8.2

In a two-neck round bottom flask (250 mL), a stock solution of 100 mL of 1 M NaOH (3.40 g, 85 mmol) was prepared in distilled water. Ferric nitrate nonahydrate **27** (1.453 g, 3.60 mmol) and ferrous sulfate heptahydrate **25** (0.50 g, 1.80 mmol) were dissolved in 12 mL and 8 mL of deoxygenated distilled water respectively. The two solutions were mixed together and sonicated for 30 min using ultra bath sonicator. After sonication, the mixture was added slowly to 1 M NaOH (100 mL) solution at room temperature with vigorous stirring. The reaction mixture was heated at 80 °C for 1 h under N_2 atmosphere. After 30 min, the reaction mixture was cooled to ambient temperature. The brown-black precipitate was washed five times with distilled water (5 × 5 mL) and then with absolute ethanol (5 mL) followed by magnetic decantation. The precipitate was dried under reduced pressure at room temperature for 24 h.

3.8.3

In a two-neck round bottom flask (250 mL), a stock solution of 100 mL of 2M NaOH (2.308 g, 57.5 mmol) was prepared in distilled water. Ferrous chloride

tetrahydrate **28** (400 mg, 2.02 mmol) and ferric chloride hexahydrate **29** (540 mg, 2.02 mmol) were dissolved in 12 mL and 8 mL of distilled water respectively. The two solutions were mixed, and the mixture was sonicated for 30 min using ultra bath sonicator. After sonication, the mixture was added slowly to 2M NaOH (100 mL) solution at room temperature with vigorous stirring. The reaction mixture was heated at 70 °C for 30 min with vigorous stirring under N_2 atmosphere. After 30 min, the reaction mixture was cooled to ambient temperature. The brown-black precipitate was washed five times with distilled water (5 × 5 mL) and twice with absolute ethanol (2 × 5mL) followed by magnetic decantation. The nanoparticles were dried under reduced pressure at room temperature for 24

3.8.4

In a two-neck round bottom flask (50 mL), ferrous chloride tetrahydrate **28** (73.5 mg, 0.37 mmol) and ferric chloride hexahydrate **29** (200 mg, 0.74 mmol) were dissolved in 30 mL of distilled water with vigorous stirring. 1 mL of aq. ammonia (28-30%) was added slowly to the reaction mixture with constant stirring. The reaction mixture was heated at 85 °C for 2 h under N_2 atmosphere. After 2 h, the reaction mixture was cooled to ambient temperature. The black precipitate was washed thrice with distilled water (3 × 10 mL) and absolute ethanol (2 × 5 mL) followed by magnetic decantation. The magnetic nanoparticles were dried under reduced pressure for 24 h at room temperature.

3.9. General procedure for the surface functionalization of mag@silica iron (III)oxide nanoparticles with APTES (3-aminopropyltriethoxysilane) at two different concentrations

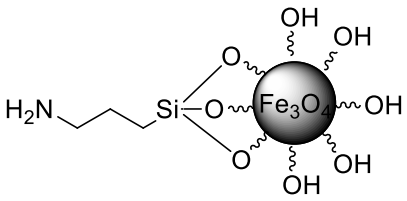

18

3.9.1. In a two-neck round bottom flask (100 mL), the mag@silica IONP were dried under vacuum at 120 °C for 6 h. The mag@silica IONP (500 mg) were dissolved in dry toluene (50 mL) with vigorous stirring at room temperature for 10 min under N_2 atmosphere. The mixture was sonicated for 1 h using ultra bath sonicator. 3-Aminopropyl triethoxysilane (0.6 mL) was added dropwise to the stirring mixture at room temperature under N_2 atmosphere. The reaction mixture was refluxed with vigorous stirring for 24 h under N_2 atmosphere. After 24 h, the reaction mixture was cooled to ambient temperature and toluene was decanted from the mixture. The precipitate was washed absolute ethanol (5 × 5 mL) followed by magnetic decantation. The precipitated APTES surface functionalized iron oxide nanoparticles **18** were dried under reduced pressure at 40 °C for 24 h [24].

3.9.2. In a two-neck round bottom flask (100 mL), the mag@silica IONP (500 mg) were dried under reduced pressure at 120 °C for 6 h. The mag@silica IONP were dissolved in distilled toluene (50 mL) with vigorous stirring at room temperature under N_2 atmosphere. The mixture was sonicated for 1 h in an ultra-bath sonicator. 3-Aminopropyl triethoxysilane (1.2 mL) was added dropwise to the stirring mixture at room temperature and the reaction mixture was heated at 60 °C for 4 days under N_2 atmosphere. After 4 days, the reaction mixture was cooled to ambient temperature and toluene was decanted slowly without disturbing the settled precipitate with the help of a magnet. The precipitate was washed with absolute ethanol (5 × 5 mL) followed by magnetic decantation. The APTES functionalized iron oxide nanoparticles **18** were dried under reduced pressure at 40 °C for 24 h.

Chapter 4

Results and Discussion

4.1 Synthesis of CA IX targeting ligand

The intended targeting ligand for CA IX receptor was synthesized starting from pentaflourobenzene sulfonyl chloride **1**. **1** on treatment with aqueous ammonia resulted in the formation of pentaflourobenzene sulfonamide **2** in an excellent 90% yield (Scheme 1).

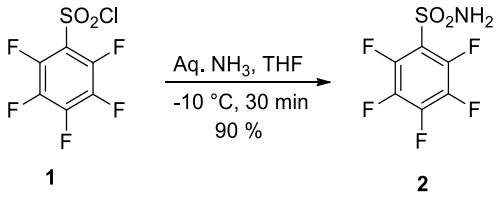

Scheme 1. Synthesis of pentaflourobenzene sulfonamide **2**

Pentaflourobenzene sulfonamide **2** was further treated with a nucleophile, such as 6-aminocaprylic acid, under optimized reaction conditions to form 4-aminocaprylic-tetrafluorosulfonamide **4** in good yield (Scheme 2, Table 1). The most accessible position for the nucleophile to attack is *para* due to favorable electronic and unfavorable steric effects. Under optimized conditions, the aromatic nucleophilic substitution reaction was facile a *para* position of **2** resulting in the formation of desired product **4** in 62% yield. Table 1 shows the effect of polarity of solvent, equivalents of base and temperature on the formation and yield of **4**. In non-polar solvent such as toluene at higher temperature, aromatic nucleophilic substitution reaction in **2** fails to take place without the formation of product **4** (Entry 1, Table 1). Whereas with the increase in the polarity of the solvent and temperature, formation of **4** was observed albeit in poor yields of 20-24% (Entries 2 and 3, Table 1). Surprisingly, when the reaction was carried out in high polar solvent such as DMSO at 80 °C, the aromatic nucleophilic substitution at *para* position of **2** was facile and the desired product **4** was obtained in a good yield of

62% (Entry 4, Table 1). The number of equivalents of base had minimum effect in the conversion of **2** to **4** and a minimum of 1.0 equivalent of base such as Et_3N was enough to afford **4** in good yield (Entry 4, Table 1).

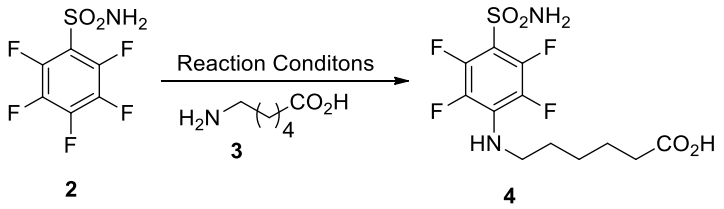

Scheme 2. Synthesis of 4-aminocaprylictetrafluorosulfonamide **4**

Entry	Reaction Conditions	% Yield **4**
1.	**3 (**1.1 equiv.), Toluene, Et_3N (1.01 equiv.), 80 ℃, 24 h	_
2.	**3 (**1.1 equiv.), THF, Et_3N (1.01 equiv.), 70 ℃, 8 h	20
3.	**3 (**1.1 equiv.), Methanol, Et_3N (1.01 equiv.), 65 ℃, 16 h	24
4.	**3 (**1.1 equiv.), DMSO, Et_3N (1.01 equiv.), 80 ℃, 24 h	62

Table 1. Optimization of reaction conditions for the preparation of **4**

4-Substituted-2,3,5,6-tetraflourobenzene sulfonamide **4** is still activated for further aromatic nucleophilic substitution reaction in the *ortho* position of the sulfonamide functional group. Accordingly, when **4** was treated with cyclooctyl amine **5** (1.1 equiv.), and a base, Et_3N (1.0 equiv.) the ortho fluorine substituent in **4** underwent substitution by the amino nucleophile, cyclooctyl amine **5**, to afford 2,4-diaminosubstituted-3,5,6-triflourobenzene sulfonamide **6** in a poor yield of 24% yield (Scheme 3, Table 2). The substation pattern can be explained by the fact that the most accessible site for the nucleophilic attack in **4** is either C2–F or C6–F positions and not C3–F or C5–F positions. The C2–F or C6–F positions of **4** are relatively more electron deficient compared to C3–F or C5–F positions because of presence of 4-amino substituent. The yield of formation of **6** was also improved by increasing the number of equivalents of nucleophile (2.0 equiv.) along with base (2.0

equiv) . Further, **6** could be used as a new small molecule targeting ligand to target CA IX receptor overexpressed in the hypoxic solid tumors that was not explored before.

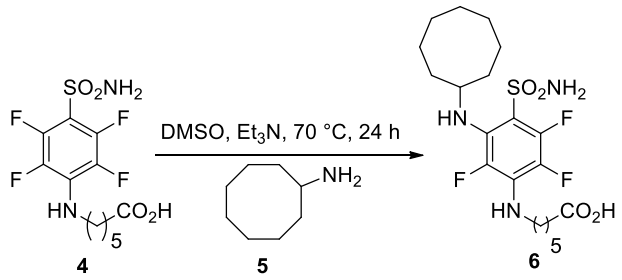

Scheme 3. Synthesis of new small molecule ligand **6** to target CA IX receptor

Entry	Reaction conditions	% Yield 6
1.	**5 (**1.1 equiv.), DMSO, Et_3N (1.01 equiv.), 70 ℃, 24 h	24
2.	**5** (2.0 equiv.), DMSO, Et_3N (2.0 equiv.), 70 ℃, 24 h	32

Table 2. Optimization of reaction conditions for the preparation of CA IX targeting ligand **6**

4.2 Synthesis of biconjugate linker 11 for delivery of fluorescent reporter, Bodipy to hypoxic tumors

Next, we carried out the conjugation of targeting ligand **6** with appropriate peptidic spacer using solid phase peptide synthesis (SPPS) methodology to prepare the biconjugate linker **11** which could be attached to a fluorescent reporter, Bodipy dye, for drug delivery applications to hypoxic tumors over-expressing CA IX receptors. The free amine group of 1,2-diaminoethanetrityl resin **7** was coupled with the carboxylic acid group of the PEG linker **8** using HATU as coupling reagent and DIPEA as a base for the activation of acid group resulting in the formation of dipeptide **9**. The NHFmoc group in **9** was deprotected using 20% piperidine in DMF to afford free amino group in the dipeptide chain **9** which was coupled with the CA IX targeting ligand **6** to afford the targeting ligand attached peptide chain

10. The ligand conjugated PEG spacer **10** was cleaved from the resin with the help of TFA/EDT/TIS/H_2O cleavage cocktail (92.5:2.5:2.5:2.5) to afford **11** in 68% yield. The targeted bioconjugate **11** with free amino group would be attached later to a fluorescent reporter, Bodipy, to detect hypoxic tumors in an early stage which is currently in progress in our laboratory (Scheme 4).

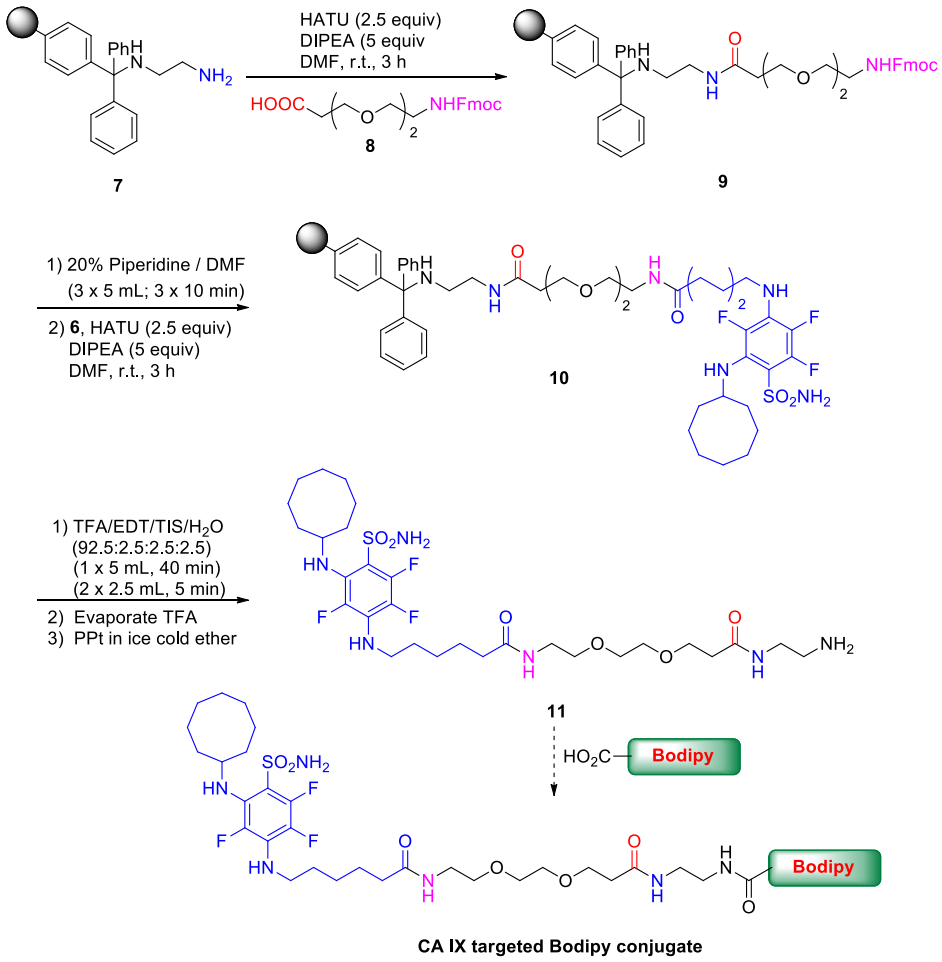

Scheme 4. Synthesis of CA IX targeted Bodipy conjugate containing PEG spacer for drug delivery applications

4.3 Synthesis of CA IX targeted ligand conjugate 16 with cysteine terminus for attaching functionalized iron oxide nanoparticles

With the aim of detection and treatment of hypoxic tumors using releasable iron oxide nanoparticles by the principle of MRI and hyperthermia we begin the

synthesis of bioconjugate linker **16** which can be later attached to iron oxide nanoparticles. The iron oxide nanoparticles can be used both as MRI contrast agent as well as therapeutic agent to target hypoxic tumors overexpressing CA IX receptors. First, we plan to conjugate the targeting ligand **6** with appropriate peptidic spacer using solid phase peptide synthesis (SPPS) methodology to prepare the biconjugate linker **16** with cysteine terminus that can be attached to functionalized iron nanoparticles.

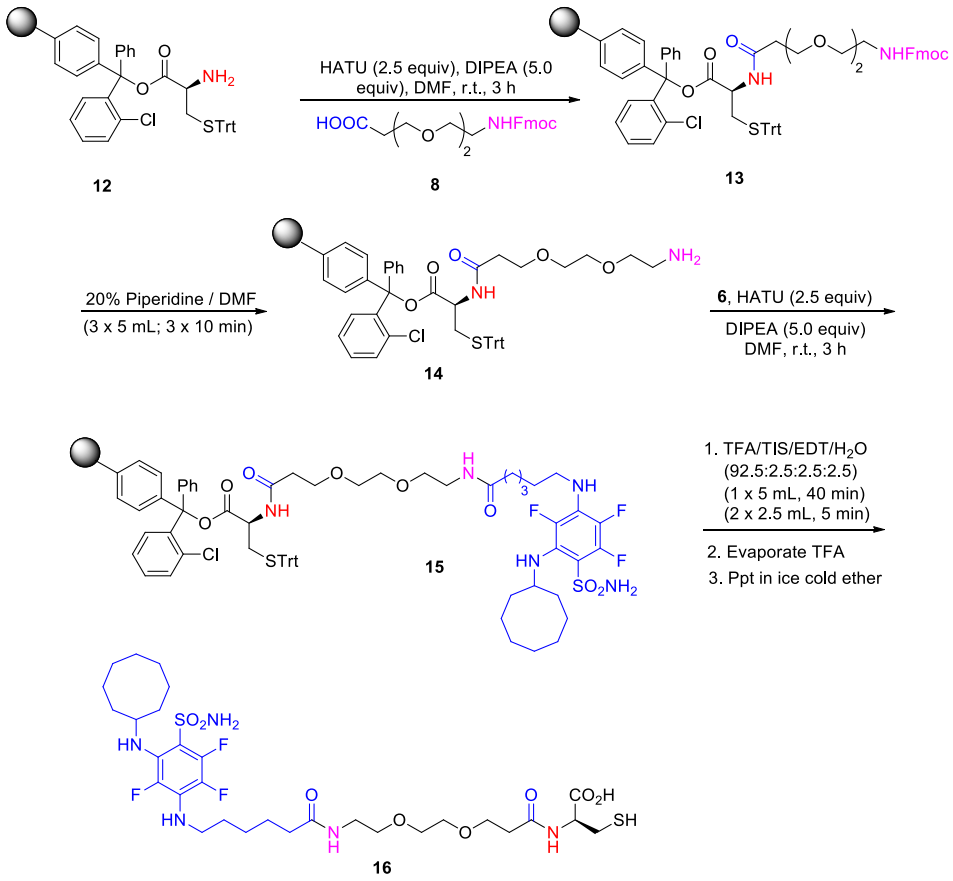

Scheme 5. Synthesis of CA IX targeted ligand conjugate 1**6** with cysteine terminus for attaching functionalized iron oxide nanoparticles

Briefly, the free amine group of H-Cys(Trt)-2-chlorotrityl resin **12** was coupled with the carboxylic acid group of the PEG linker **9** using HATU as coupling reagent and DIPEA as a base for the activation of acid group to afford a dipeptide **13.** The NHFmoc group in the dipeptide **13** was deprotected using 20% piperidine in DMF

to afford free amino group in the dipeptide **14** which was coupled with CA IX targeting ligand **6** to afford targeting ligand attached peptide conjugate **15**. The cleavage of targeted ligand conjugate **15** from the resin was carried out using a cleavage cocktail of TFA/EDT/TIS/H_2O (92.5:2.5:2.5:2.5) to obtain the bioconjugate linker **16** in a good yield of 62% (Scheme 5).

4.4 Synthesis of functionalized self-immolative disulfide iron oxide nanoparticles 20 and conjugation with CA IX targeted bioconjugate 16

Iron oxide nanoparticles **17** prepared by standard procedure as described below will be coated with silica to produce mag@silica iron oxide nanoparticles which will be functionalized with 3-aminopropyltriethoxysilane (APTES) silanizating agent to afford surface functionalized iron nanoparticles **18**. The free amino group in **18** will be conjugated with NHS ester **19** of 3-(pyridin-2-yldisulfanyl)propanoic acid **24** to provide disulfide activated iron oxide nanoparticles **20** (Scheme 6).

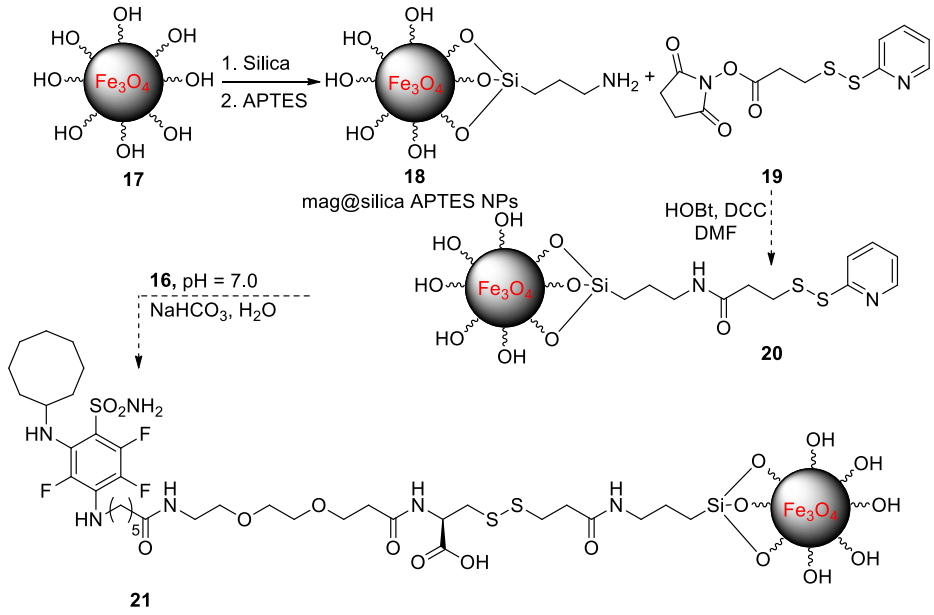

Scheme 6. Synthesis of disulfide activated iron oxide nanoparticles **20** and its conjugation with CA IX targeted hydrophilic cysteine linker **16**

4.4.1 Synthesis of N-succinimidyl-3-(2-pyridyldithio)propionate 19

N-Succinimidyl-3-(2-pyridyldithio)propionate (SPDP) **19** was prepared by following a two-step procedure as shown in scheme 7. First, 3-mercaptopropanoic acid was reacted with dipyridyl disulfide **22** by a thiol-disulfide exchange in a solution of anhydrous ethanol under the acetic acid condition to afford 3-(2-pyridyldithio)propanoic acid **19** in 72% yield. The side reaction of **19** undergoing thio-disulfide exchange with 3-mercaptopropanoic acid was completely suppressed by using a 2-fold molar excess of **22**. The pyridyldithiopropionic acid **24** was then converted to **19** by esterification with N-hydroxysuccinamide using *N*,*N*-dicyclohexylcarbodiimide (DCC) in 70% yield after column purification (Scheme 7).

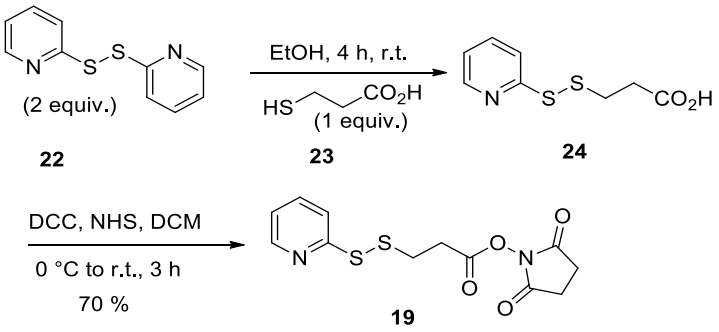

Scheme 7. Synthesis of N-succinimidyl-3-(2-pyridyldithio)propionate **19**

4.4.2 Synthesis of supermagnetic iron oxide nanoparticles 17 and surface functionalization to 18 for bioconjugation

The supermagnetic iron oxide nanoparticles **17** were prepared by co-precipitation method using various reaction conditions (Scheme 8, Eq.1-4). However, the iron oxide nanoparticles prepared are unstable under aerobic condition and gets oxidized to Fe_2O_3 resulting in agglomeration.

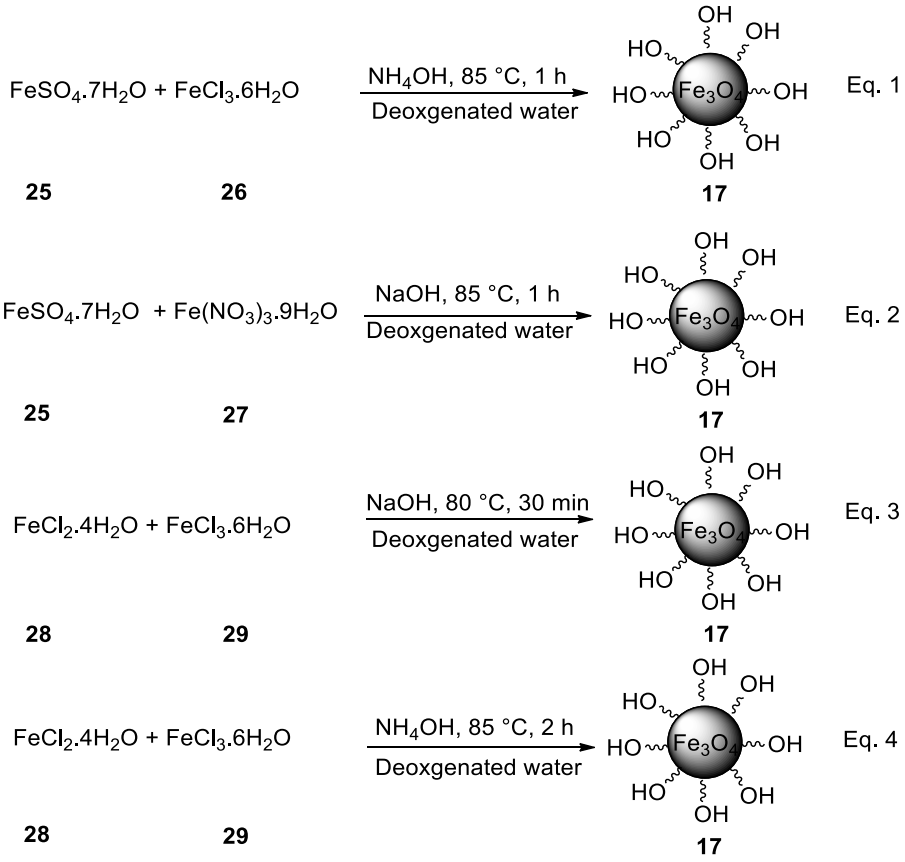

Scheme 8. Optimized reaction conditions for the preparation of iron oxide nanoparticles **17**

The better method to prevent the oxidation and agglomeration is to coat the surface of iron oxide nanoparticles with silica. APTES (3-aminopropyltriethoxy silane) is widely used for the surface functionalization of iron oxide nanoparticles. Initially the surface of the unstable iron oxide nanoparticles was coated with silica as per patented procedure (confidential) reported from the research group of Andreas *et al* in Leibniz University of Hannover, Germany, to produce mag@silica iron oxide nanoparticles and later functionalized using APTES to form surface functionalized mag@silica nanoparticles (Scheme 9). The surface functionalized mag@silica nanoparticles will be used for further conjugation to CA IX targeted bioconjugate with cysteine terminus **16** to afford **21** which is currently underway in our laboratory (Scheme 9).

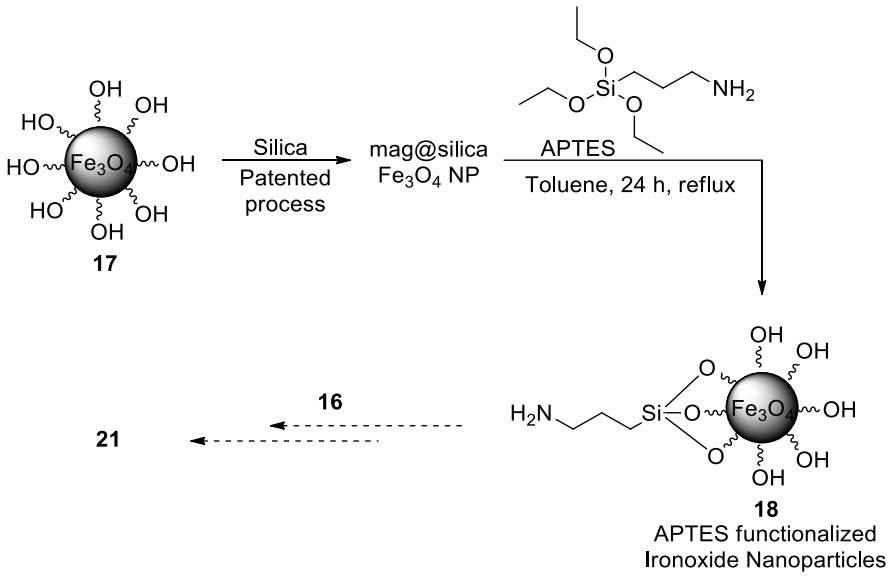

Scheme 9. Surface modification of mag@silica iron oxide nanoparticles with APTES to form surface functionalized iron oxide nanoparticles **18**

Chapter 5

Conclusion

In this research work, we have successfully synthesized a new sulfonamide CA IX targeting ligand **6** in three-steps with 32% yield. The CA IX targeting ligand **6** was conjugated with appropriate peptidic spacer using solid phase peptide synthesis (SPPS) methodology and the biconjugate linker **11** was prepared in good yield which could be attached to a fluorescent reporter, Bodipy, for drug delivery applications to hypoxic tumors over-expressing CA IX receptors.

Also, for the detection and treatment of hypoxic tumors using releasable iron oxide nanoparticles by the principle of MRI and hyperthermia, we have also synthesized a bioconjugate linker **16** using SPPS methodology which can be later attached to iron oxide nanoparticles. The iron oxide nanoparticles can be used both as MRI contrast agent as well as therapeutic agent to target hypoxic tumors overexpressing CA IX receptors.

In addition, iron oxide nanoparticles **17** were prepared by standard procedure as described before and coated with silica to produce mag@silica iron oxide nanoparticles. The silica coated iron oxide nanoparticles were also functionalized with 3-aminopropyltriethoxysilane (APTES), a silanizating agent, to provide surface functionalized iron oxide nanoparticles **18**.

The surface functionalized iron oxide NP's **18** would be converted to disulfide activated iron oxide nanoparticles **20**. Disulfide activated iron oxide nanoparticles **20** would be conjugated with CA IX targeted hydrophilic cysteine linker **16** to give the releasable iron oxide nanoparticle CA IX bioconjugate **21** for detection and treatment of hypoxic tumors in future.

APPENDIX–A

^{1}H, ^{13}C, ^{19}F NMR and Mass Spectra

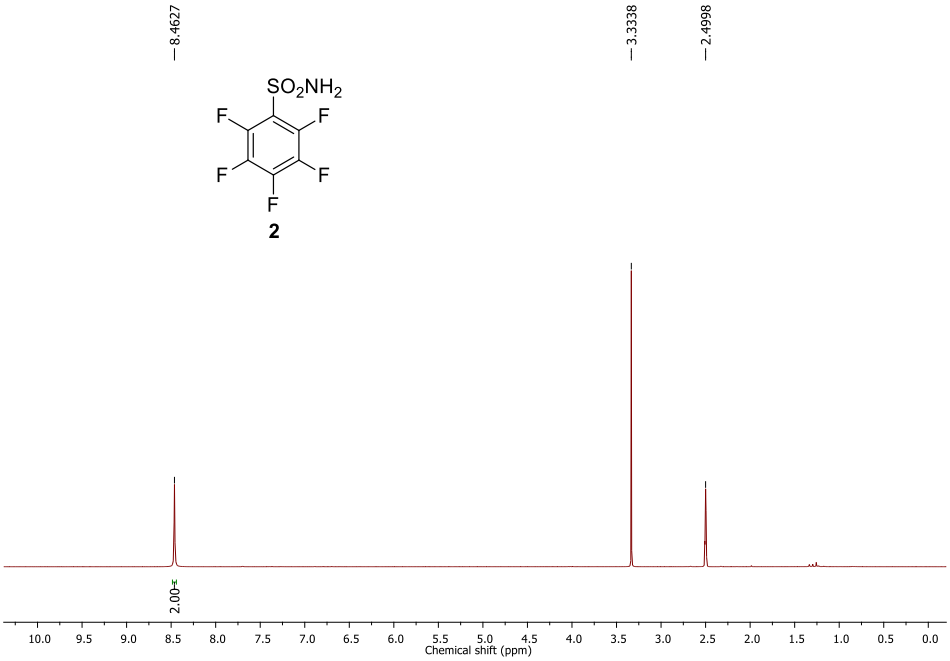

Figure 2. ^{1}H NMR spectrum of pentaflourobenzene sulfonamide **2** in DMSO-d_6

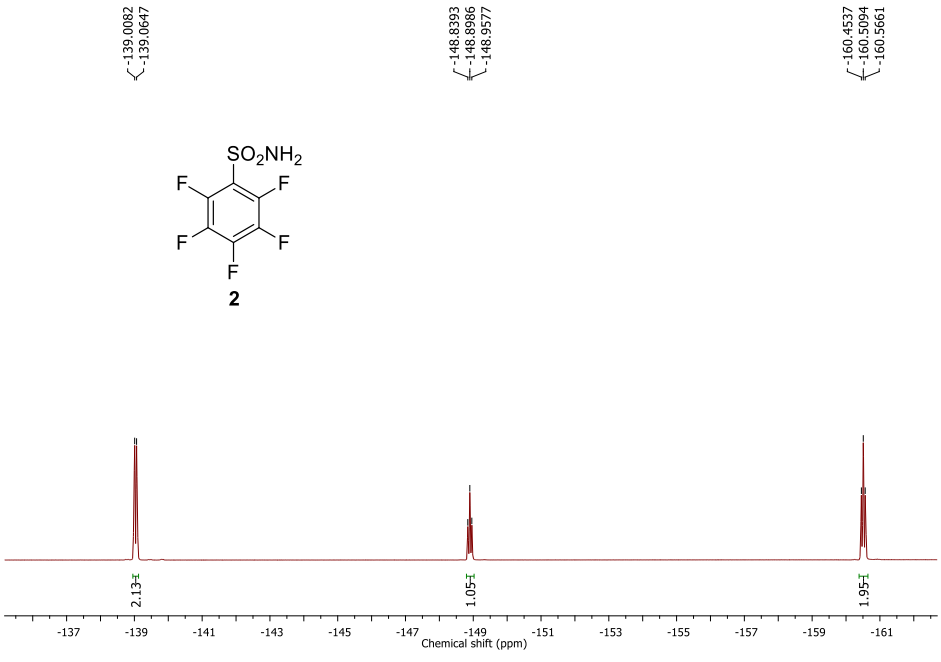

Figure 3. ^{19}F NMR spectrum of pentaflourobenzene sulfonamide **2** in DMSO-d_6

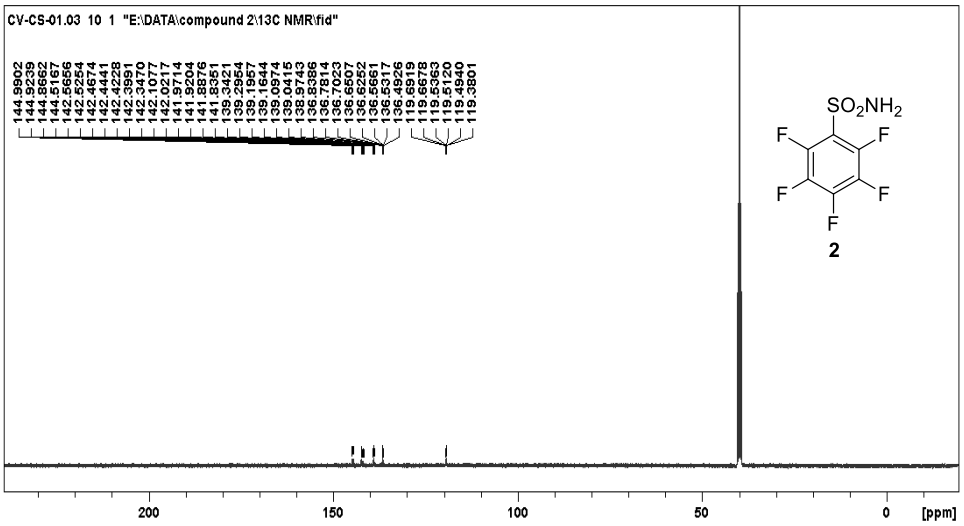

Figure 4. ^{13}C NMR spectrum of pentaflourobenzene sulfonamide **2** in DMSO-d_6

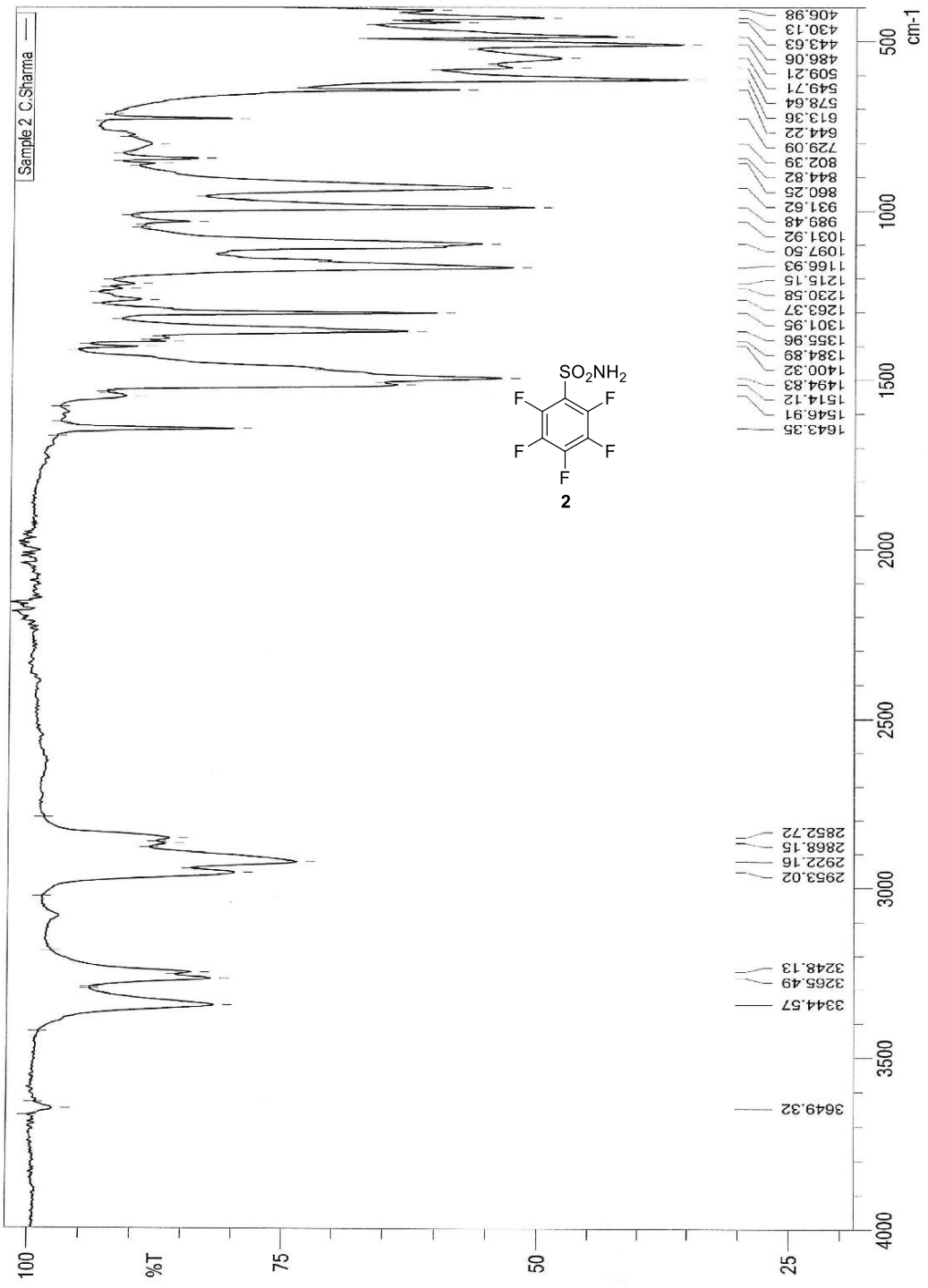

Figure 5. IR spectrum of pentaflourobenzene sulfonamide **2**

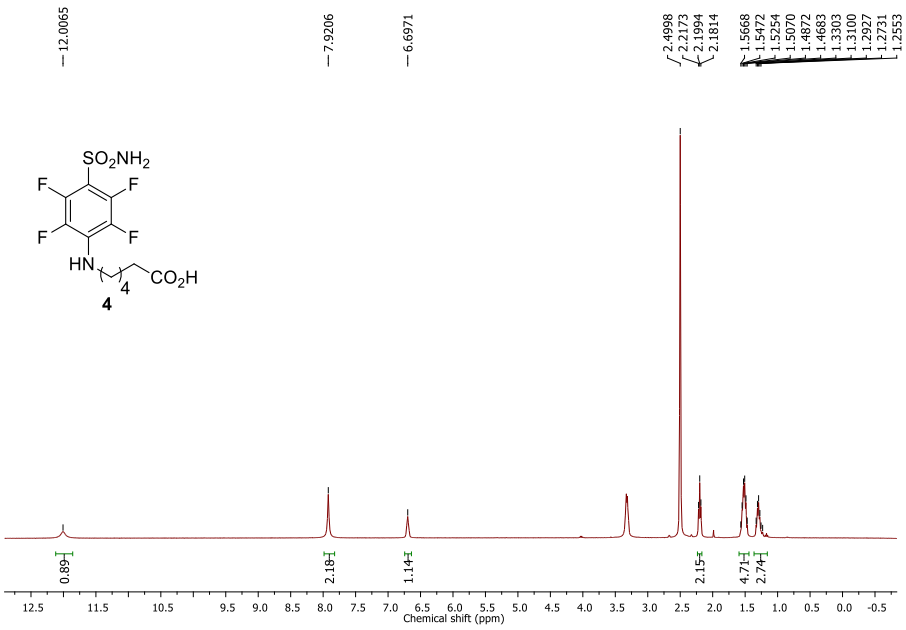

Figure 6. ^{1}H NMR spectrum of 4-aminocaprylictetraflourosulfonamide **4** in DMSO-d_6

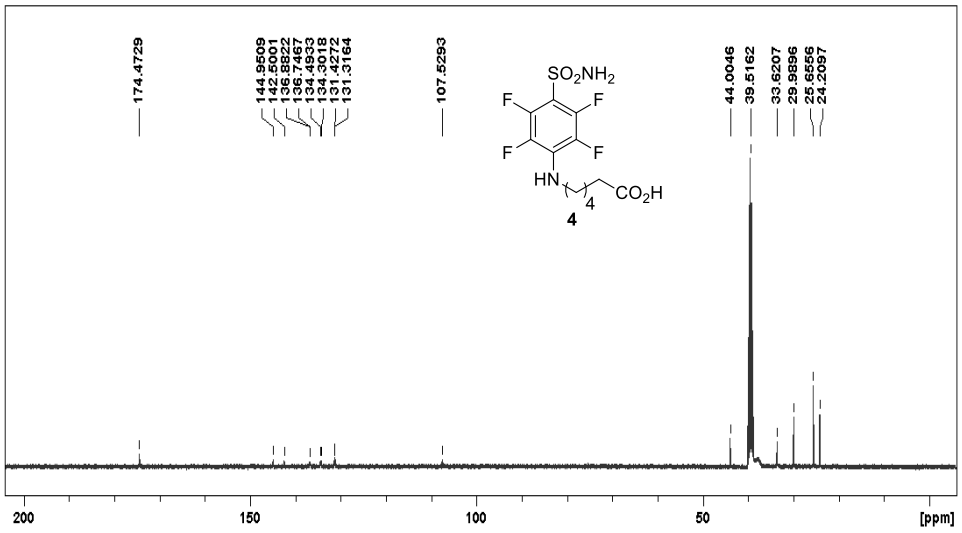

Figure 7. ^{13}C NMR spectrum of 4-aminocaprylictetraflourosulfonamide **4** in DMSO-d_6

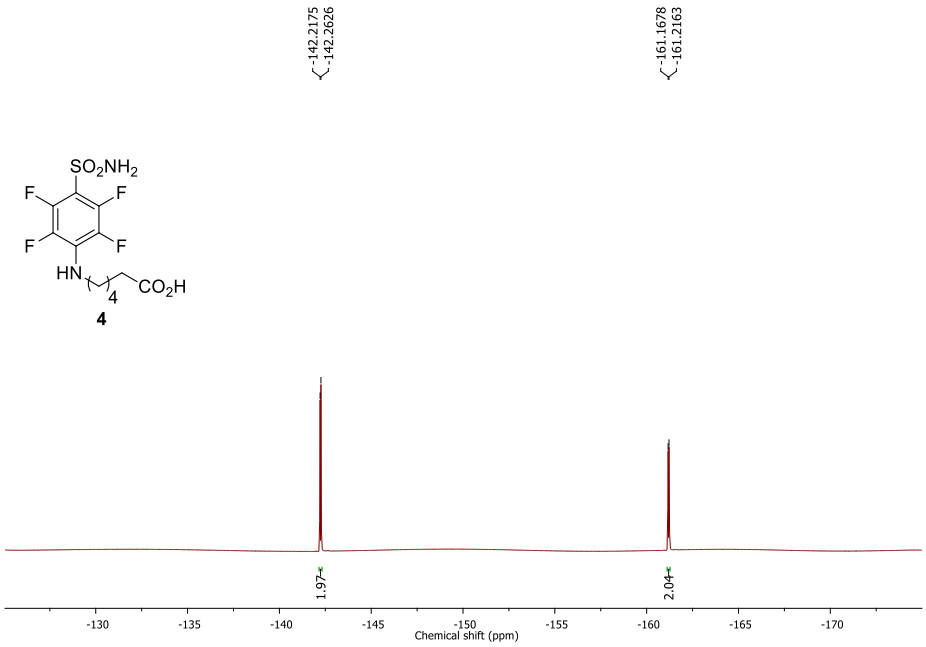

Figure 8. ^{19}F NMR spectrum of 4-aminocaprylictetraflourosulfonamide **4** in DMSO-d_6

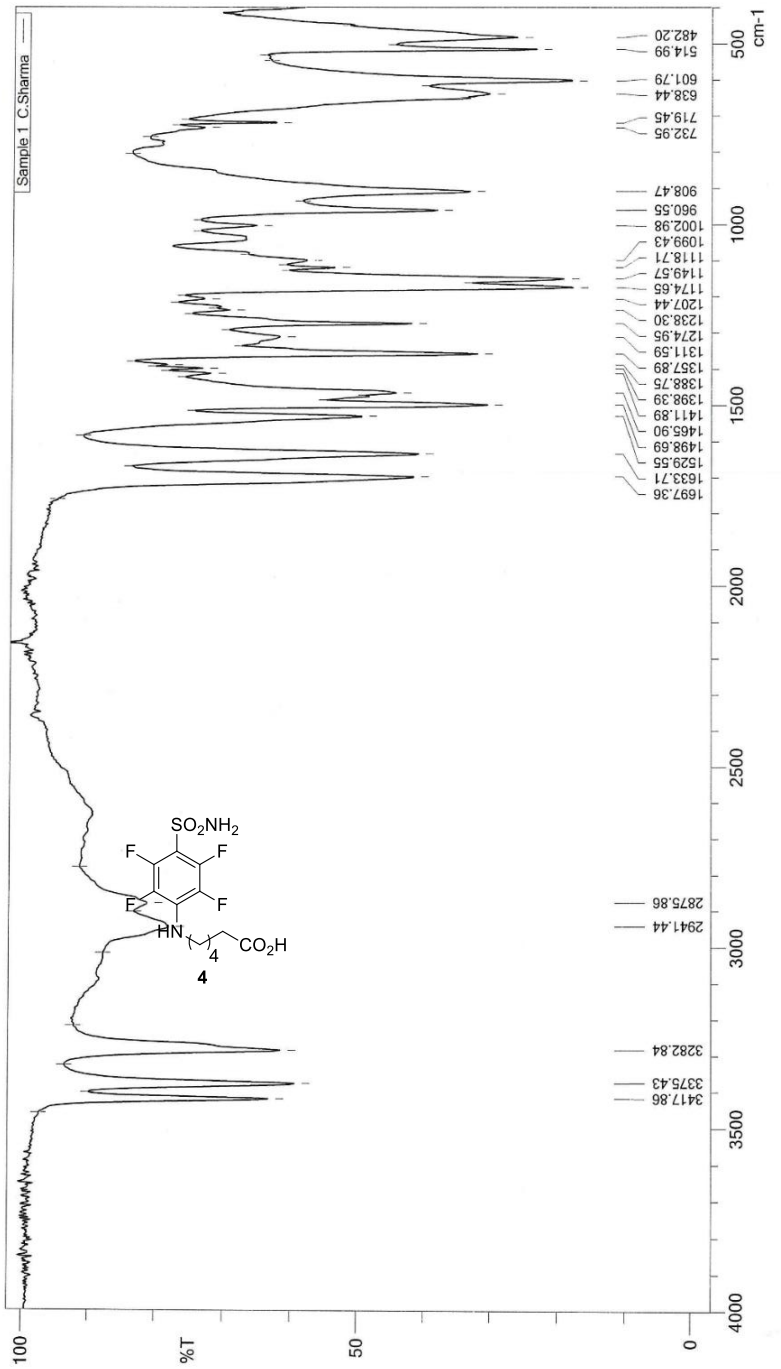

Figure 9. IR spectrum of 4-aminocaprylictetraflourosulfonamide **4**

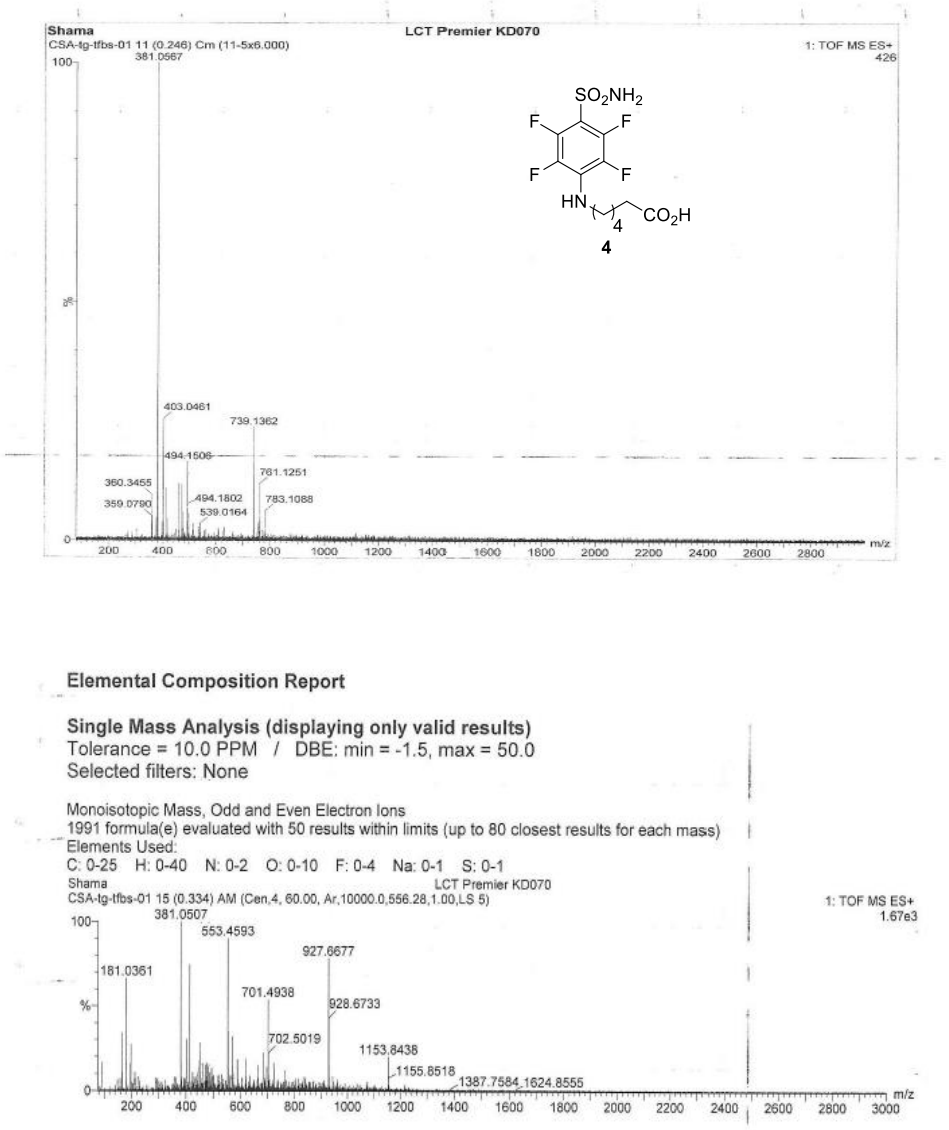

Figure 10. HR-MS of 4-aminocaprylictetraflourosulfonamide **4**

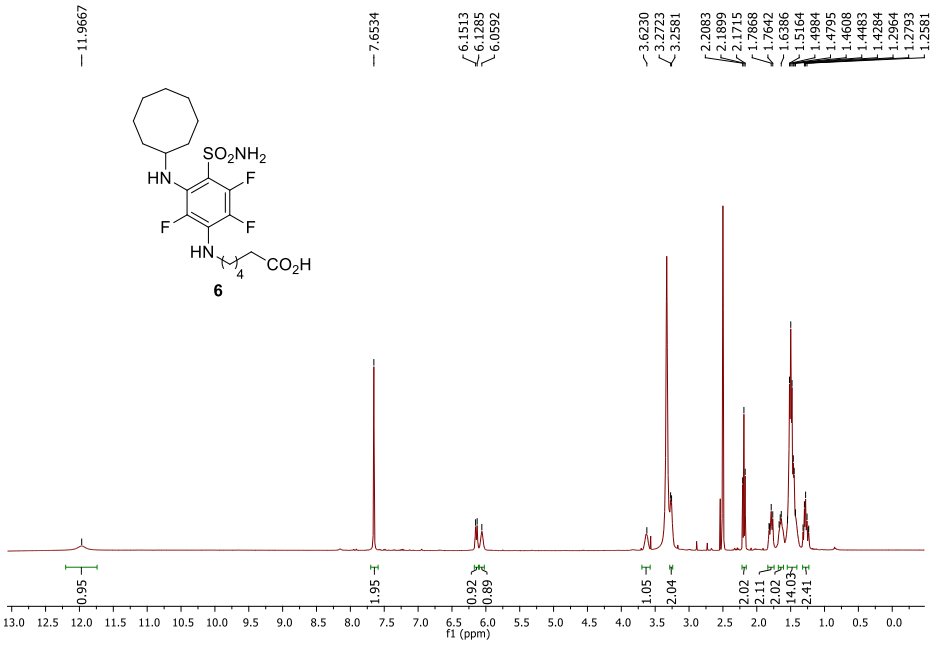

Figure 11. ^{1}H NMR spectrum new small molecule ligand to target CA IX receptor **6** in DMSO-d_6

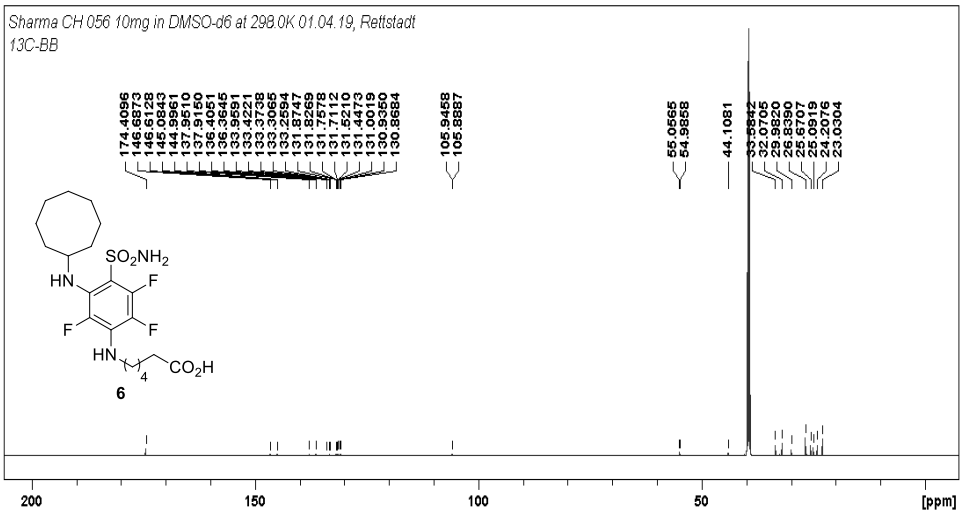

Figure 12. ^{13}C NMR spectrum of new small molecule ligand to target CA IX receptor **6** in DMSO-d_6

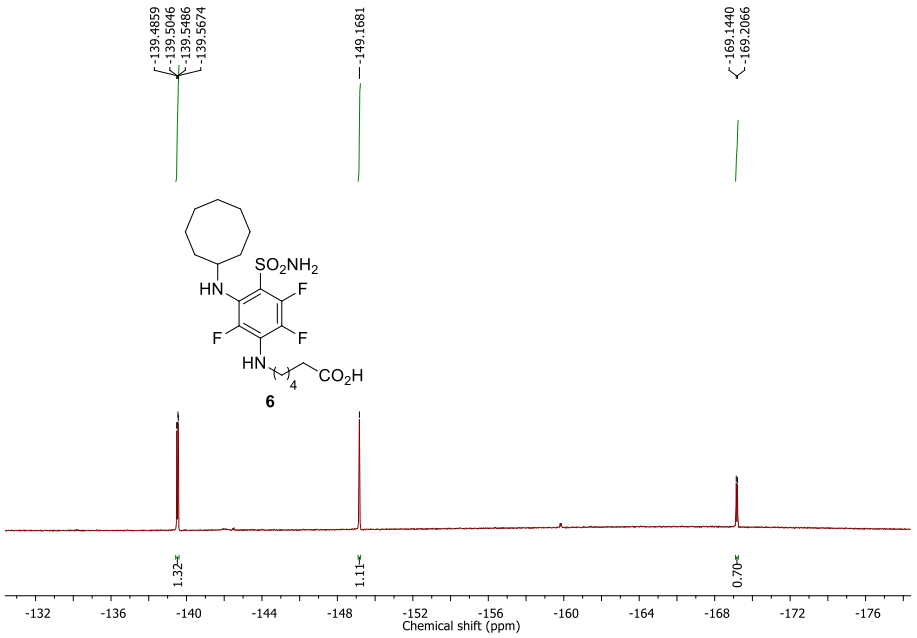

Figure 13. ^{19}F NMR spectrum of new small molecule ligand to target CA IX receptor **6** in DMSO-d_6

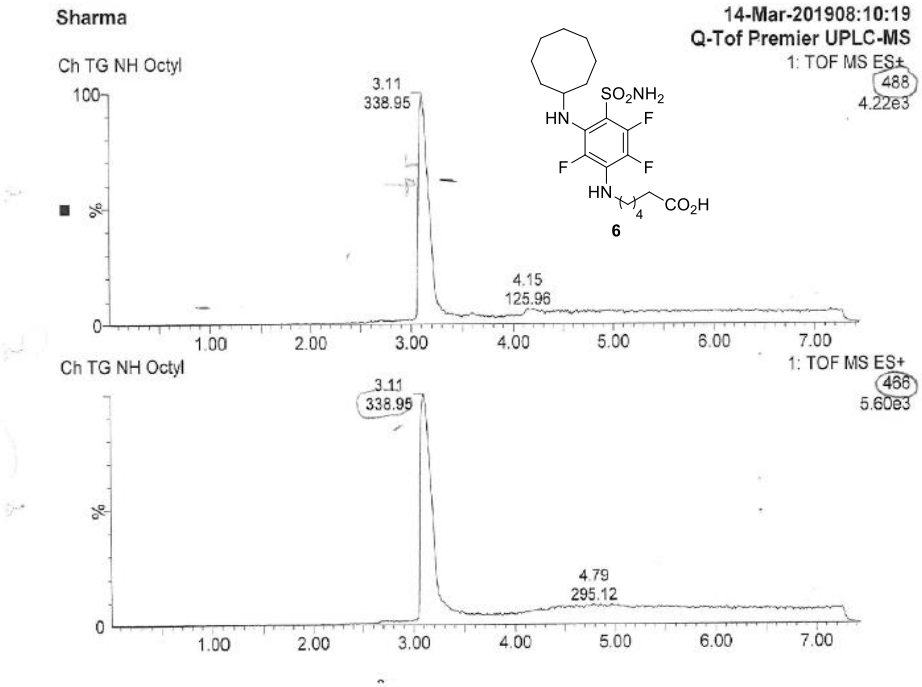

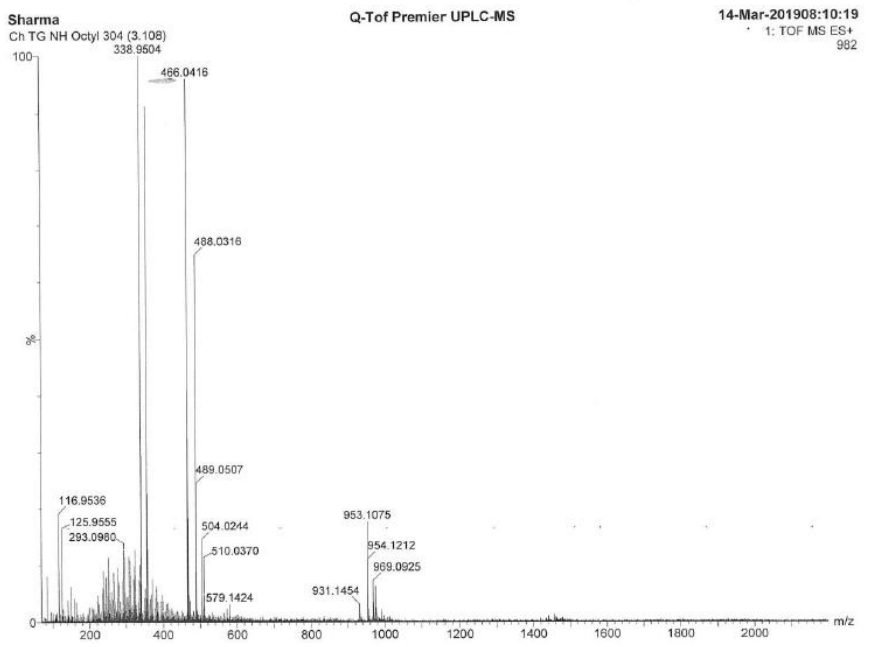

Elemental Composition Report

Single Mass Analysis
Tolerance = 20.0 PPM / DBE: min = -0.5, max = 50.0
Selected filters: None

Monoisotopic Mass, Even Electron Ions
1860 formula(e) evaluated with 37 results within limits (all results (up to 1000) for each mass)
Elements Used:
C: 0-60 H: 0-60 N: 0-3 O: 0-5 Na: 0-1 S: 0-1 F: 0-3

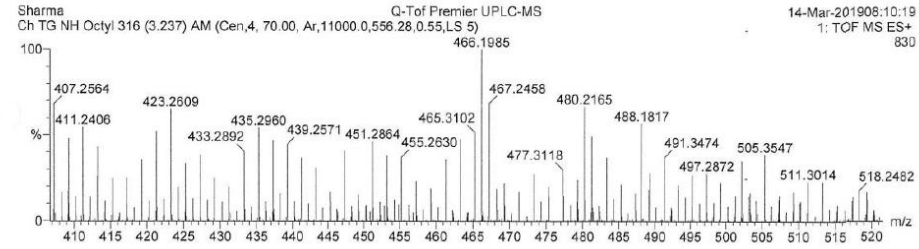

Figure 14. HR-MS of new small molecule ligand to target CA IX receptor **6**

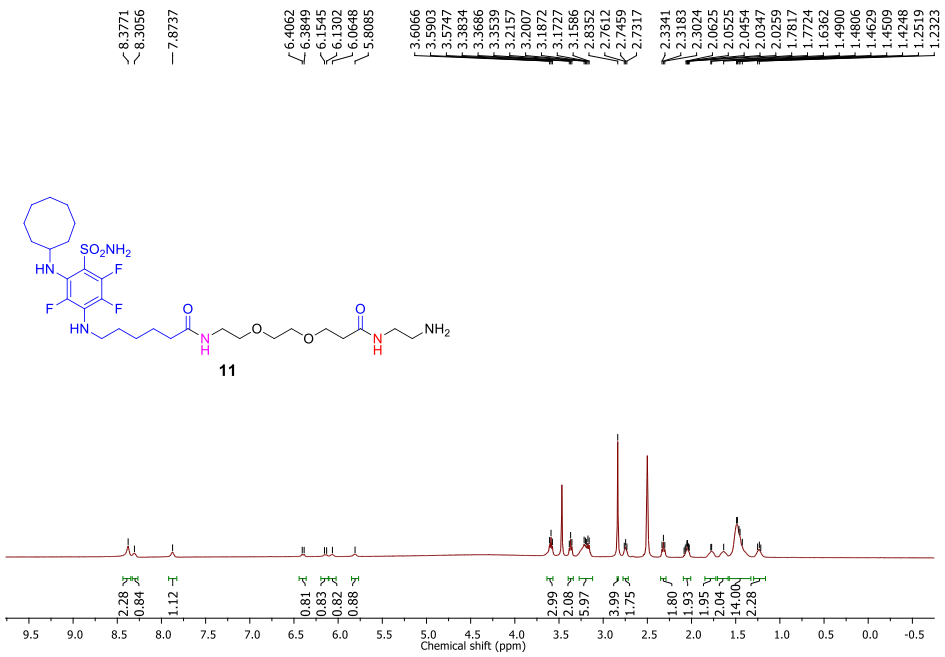

Figure 15. ^{1}H NMR spectrum of CA IX targeting ligand **6** conjugated PEG spacer **11** in DMSO-d_6

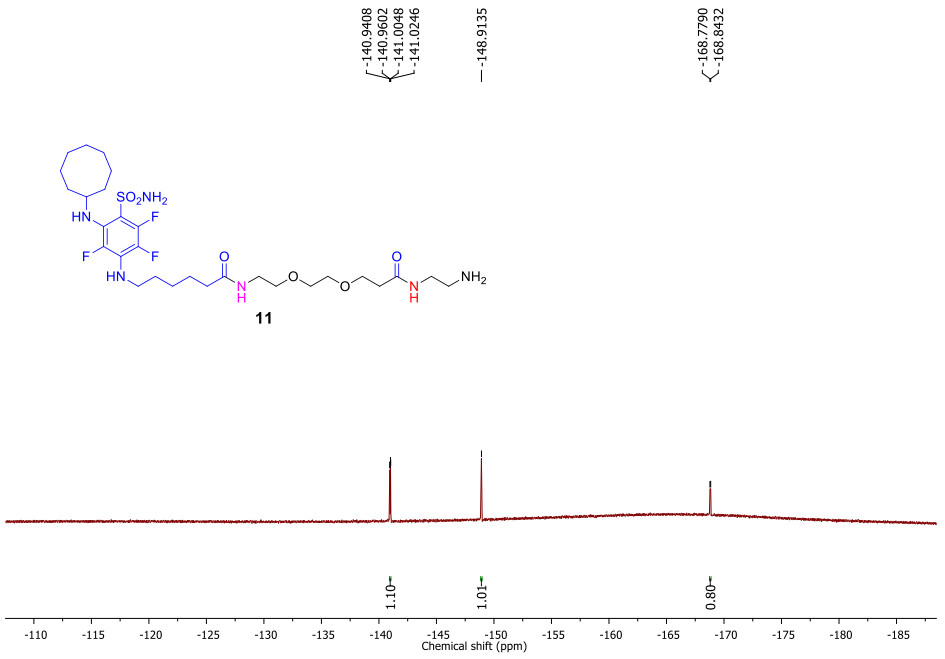

Figure 16. ^{19}F NMR spectrum of CA IX targeting ligand **6** conjugated PEG spacer **11** in DMSO-d_6

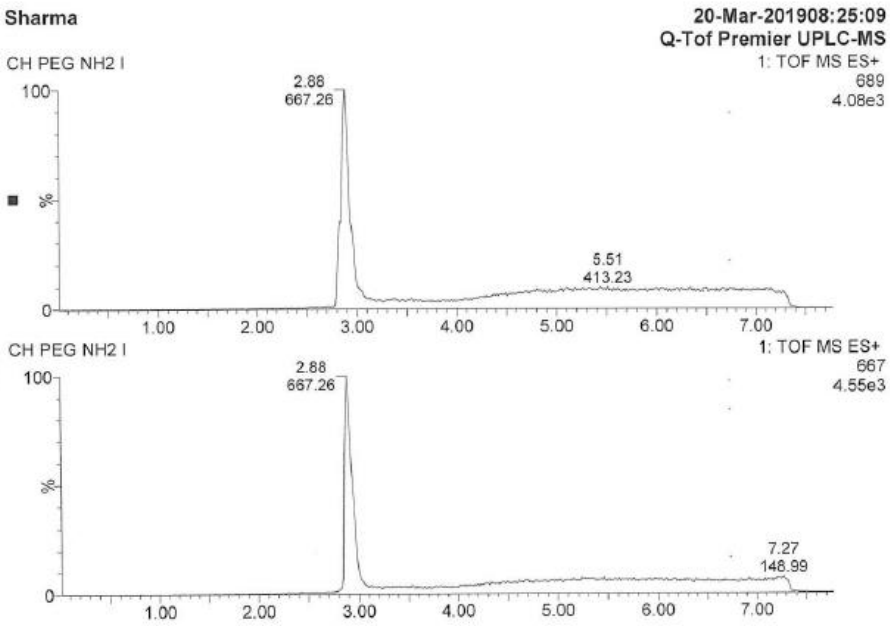
Sharma
20-Mar-201908:25:09
Q-Tof Premier UPLC-MS
CH PEG NH2 I
1: TOF MS ES+
689
4.08e3
2.88
667.26
5.51
413.23
100
%
0
1.00
2.00
3.00
4.00
5.00
6.00
7.00
CH PEG NH2 I
1: TOF MS ES+
667
4.55e3
2.88
667.26
7.27
148.99

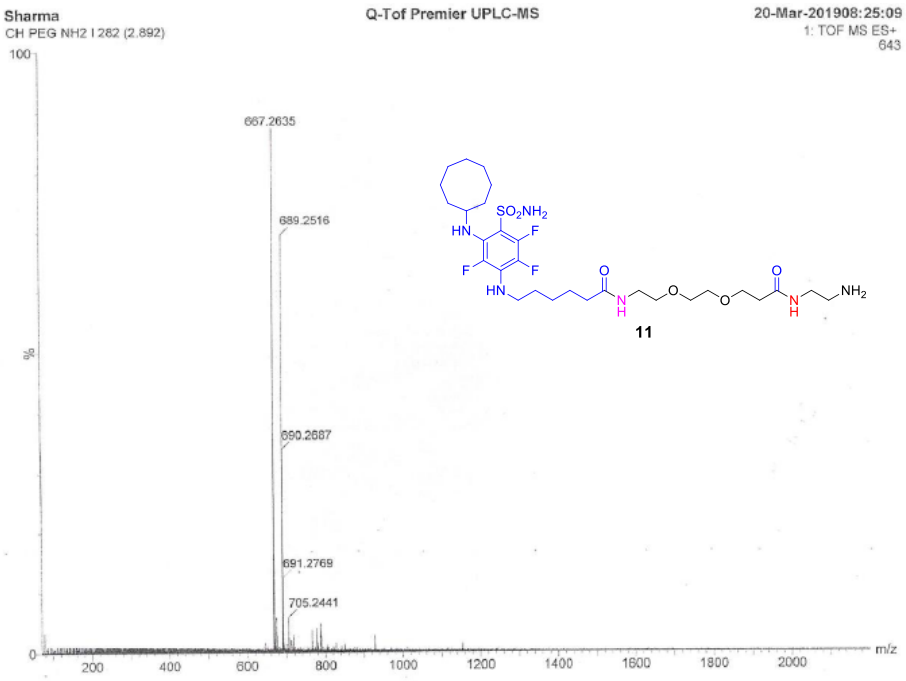
Sharma
CH PEG NH2 I 282 (2.892)
Q-Tof Premier UPLC-MS
20-Mar-201908:25:09
1: TOF MS ES+
643
667.2635
689.2516
690.2687
691.2769
705.2441
m/z
200
400
600
800
1000
1200
1400
1600
1800
2000

11

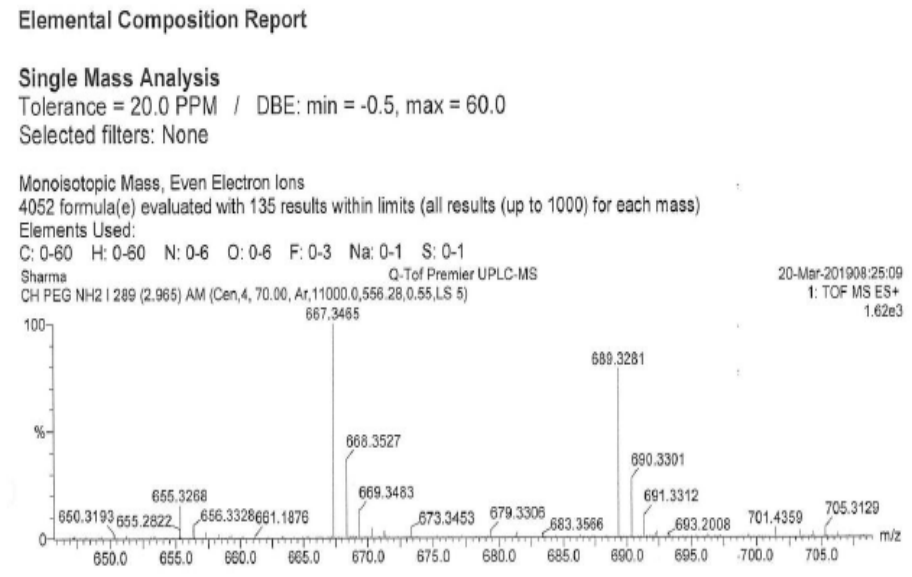

Figure 17. HR-MS of CA IX targeting ligand **6** conjugated PEG spacer **11** in DMSO-d_6

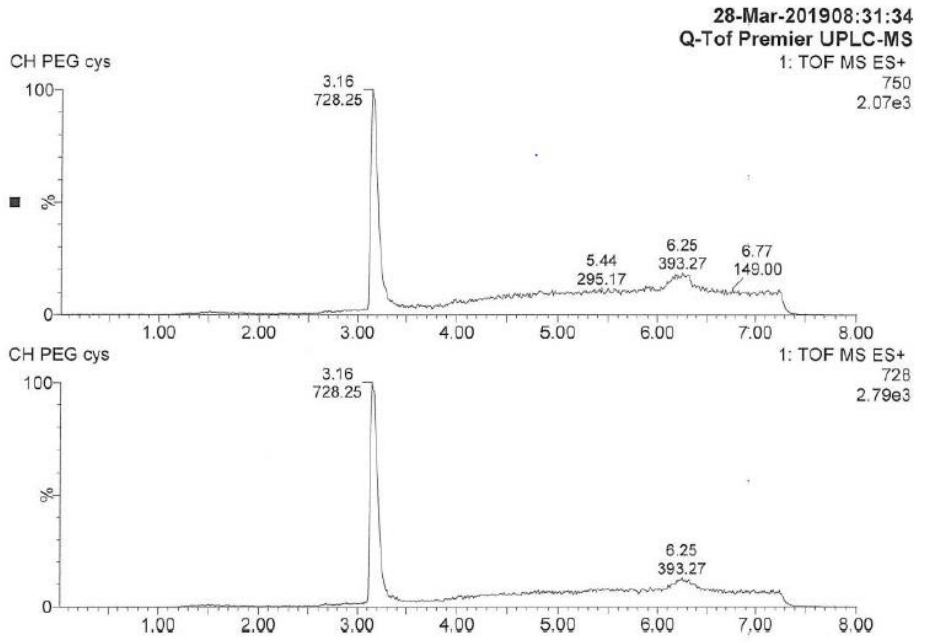

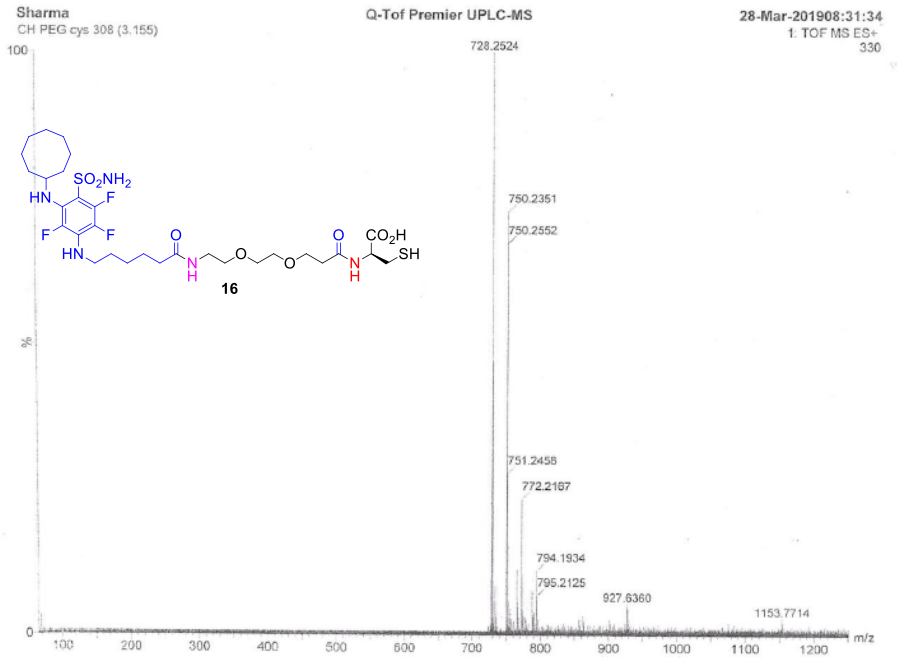

Elementcl Composition Report

Single Mass Analysis
Tolerance = 20.0 PPM / DBE: min = -0.5, max = 60.0
Selected filters: None

Monoisotopic Mass, Even Electron Ions
7807 formula(e) evaluated with 209 results within limits (all results (up to 1000) for each mass)
Elements Used:
C: 0-60 H: 0-60 N: 0-6 O: 0-8 Na: 0-1 S: 0-2 F: 0-3

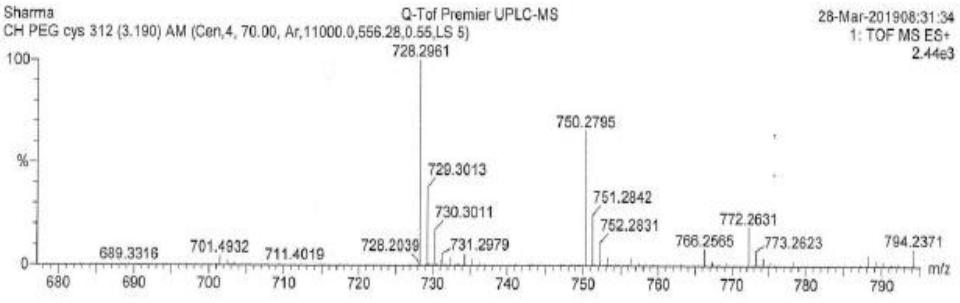

Figure 18. HR-MS of CA IX targeting ligand **6** tethered cysteine linker **16**

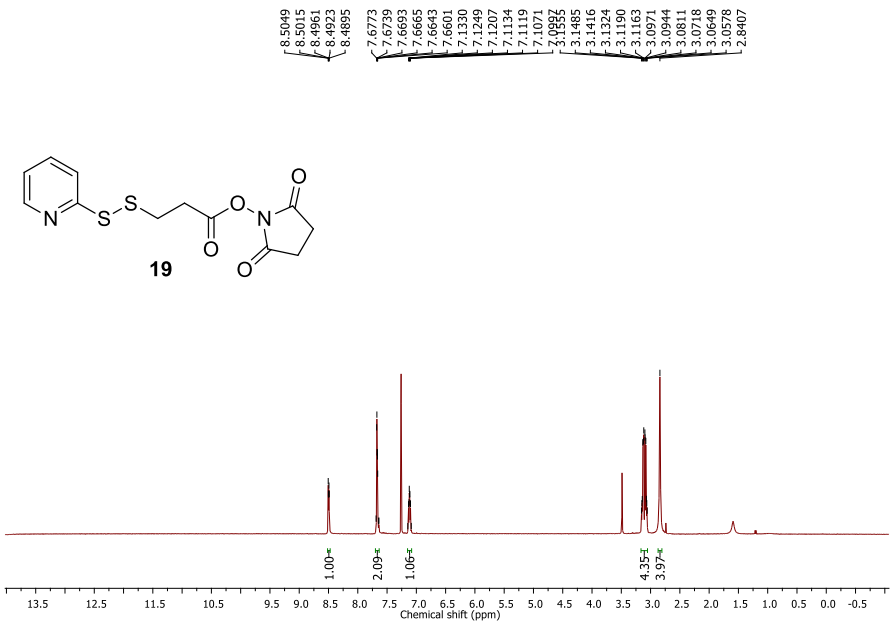

Figure 19. ^{1}H NMR spectrum of N-succinimidyl-3-(2-pyridyldithio) propionate **19** in $CDCl_3$

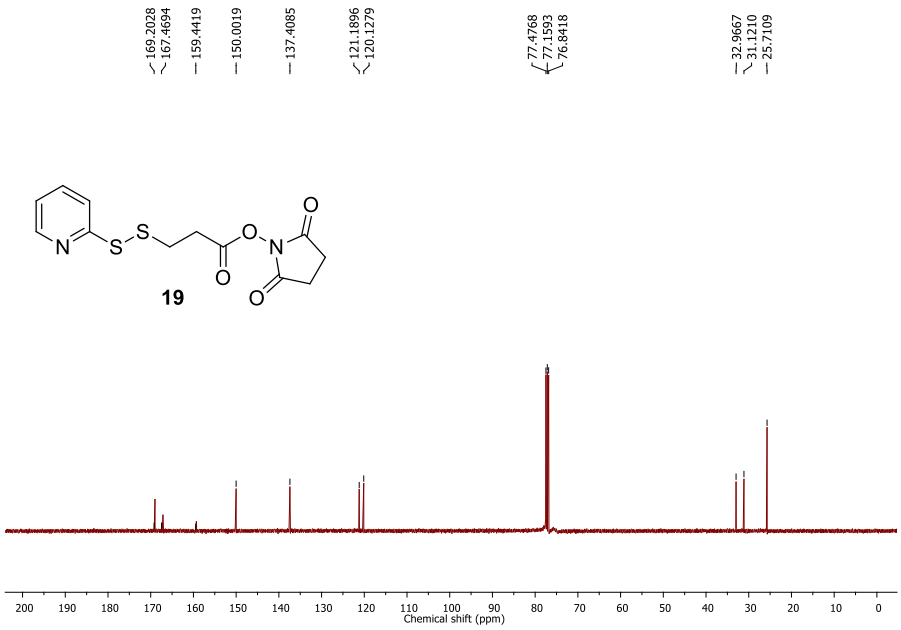

Figure 20. ^{13}C NMR spectrum N-succinimidyl-3-(2-pyridyldithio) propionate **19** in $CDCl_3$

REFERENCES

[1] Moulder, J.E., Rockwell, S. (1987), Tumor hypoxia: Its impact on cancer therapy. *Cancer Metastasis Rev.*, ***5***, 313–341.

[2] Peskin, B., Carter, M.J. (2008), Chronic cellular hypoxia as the prime cause of cancer: What is the deoxygenating role of adulterated and improper ratios of polyunsaturated fatty acids when incorporated into cell membranes? *Med. Hypotheses*, ***70***, 298–304.

[3] Wykoff, C.C., Beasley, N.J., Watson, P.H., Turner, K.J., Pastorek, J., Sibtain, A., Wilson, G.D., Turley, H., Talks, K.L., Maxwell, P.H., *et al*. (2000), Hypoxia-inducible expression of tumor-associated carbonic anhydrases. *Cancer Res.*, ***60***, 7075–7083.

[4] Chia, S.K., Wykoff, C.C., Watson, P.H., Han, C., Leek, R.D., Pastorek, J., Gatter, K.C., Ratcliffe, P., Harris, A.L. (2001), Prognostic significance of a novel hypoxia-regulated marker, carbonic anhydrase IX, in invasive breast carcinoma. *J. Clin. Oncol.*, ***19***, 3660–3668.

[5] McDonald, P.C., Winum, J.Y., Supuran, C.T., Dedhar, S. (2012), Recent developments in targeting carbonic anhydrase IX for cancer therapeutics. *Oncotarget*, ***3***, 84–97.

[6] Sadri, N., Zhang, P.J. (2013), Hypoxia-inducible factors: Mediators of cancer progression, prognostic and therapeutic targets in soft tissue sarcomas. *Cancers*, ***5***, 320–333.

[7] Aggarwal, M., Boone, C.D., Kondeti, B., McKenna., R. (2013), Structural annotation of human carbonic anhydrases. *J. Enzyme Inhib. Med. Chem.*, ***28***, 267–277.

[8] Frost, S.C. (2014), Physiological functions of the alpha class of carbonic anhydrases. *Subcell. Biochem.*, ***75***, 9–30.

[9] Neri, D., Supuran, C.T. (2011), Interfering with pH regulation in tumors as a therapeutic strategy. *Nat. Rev. Drug Discov.*, ***10***, 767–777.

[10] Li, Y., Wang, H., Oosterwijk, E., Selman, Y., Mira, J.C., Medrano, T., Shiverick, K.T., Frost, S.C. (2009), Antibody-specific detection of CAIX in breast

and prostate cancers. *Biochem. Biophys. Res. Commun.*, ***386***, 488–492.

[11] Marks, I. S., Gardeen, S. S., Kurdziel, S. J., Nicolaou, S. T., Woods, J. E., Kularatne, S. A., & Low, P. S. (2018), Development of a small molecule tubulysin B conjugate for treatment of carbonic anhydrase IX receptor expressing cancers. *Mol. Pharm.*, ***15***, 2289–2296.

[12] Pandit, A., Sengupta, S., Krishnan, M. A., Reddy, R. B., Sharma, R., Venkatesh, C. (2018), First report on 3D-QSAR and molecular dynamics-based docking studies of GCPII inhibitors for targeted drug delivery applications. *J. Mol. Struct.*, ***1159***, 179–192.

[13] Rangasamy, L., Venkatesh C., Kanduluru, A. K., Srinivasarao, M., Bandara, N. A., You, F., Orellana, E. A., Kasinski, A. L., Low, P. S. (2018), New mechanism for release of endosomal contents: Osmotic lysis via nigericin-mediated K^+/H^+ exchange. *Bioconjugate Chem.*, ***29***, 1047– 1059.

[14] Roy, J., Nguyen, T.X., Kanduluru, A.K., Venkatesh, C., Lv, W., Reddy, P.N., Low, P.S. and Cushman, M. (2015), DUPA conjugation of a cytotoxic indenoisoquinoline topoisomerase inhibitor for selective prostate cancer cell targeting. *J. Med. Chem.*, ***58***, 3094–3103.

[15] Poh, S., Venkatesh, C., Low, P. S. (2015), Comparison of nanoparticle penetration into solid tumors and sites of inflammation: studies using targeted and non-targeted liposomes. *Nanotechnol. Biol. Med*., ***10***, 1439–1449.

[16] Poh, S., Venkatesh, C., Lindsay, K., Ayala López, W., Balasubramanian, V., Putt, K. S., Low, P. S. (2017), Folate-conjugated liposomes target and deliver therapeutics to immune cells in a rat model of rheumatoid arthritis. *Nanotechnol. Biol. Med*., ***12***, 2441–2451.

[17] Poh, S., Venkatesh, C., Ayala- López, W., Putt, K. S., Low, P. S. (2018), Selective liposome targeting of folate receptor positive immune cells in inflammatory diseases. *Nanotechnol. Biol. Med*., ***14***, 1033–1043.

[18] Kularatne, S. A., Venkatesh, C., Santhapuram, H. K. R., Wang, K., Vaitilingam, B., Henne, W. A., & Low, P. S. (2010), Synthesis and biological analysis of prostate-specific membrane antigen-targeted anticancer prodrugs. *J. Med. Chem.*, ***53***, 7767-7777.

[19] Low, P. S., Balasubramanian, V., Venkatesh, C. (2010), Folate receptor alpha targeting ligands. US Provisional Application Serial No.61/428,842.

[20] Rangasamy, L., Chelvam, V., Kanduluru, A.K., Srinivasarao, M., Bandara, N.A., You, F., Orellana, E.A., Kasinski, A.L., Low, P.S. (2018), New mechanism for release of endosomal contents: osmotic lysis via nigericin-mediated K+/H+ exchange. *Bioconjugate Chem.*, ***29***, 1047-1059

[21] Kirschning, A., Kupracz, L., Hartwig, J. (2012), New synthetic opportunities in miniaturized flow reactors with inductive heating. *Chem. Lett.*, ***41***, 562–570.

[22] Mancuso, L., Knobloch, T., Buchholz, J., Hartwig, J., Möller, L., Seidel, K., Collisi, W., Sasse, F., Kirschning, A. (2014), Preparation of thermo cleavable conjugates based on ansamitocin and superparamagnetic nanostructured particles by a chemo-biosynthetic approach. *Chem. Eur. J.*, ***20***, 17541–17551.

[23] Seidel, K., Balakrishnan, A., Alexiou, C., Janko, C., Komoll, R. M., Wang, L.L., Kirschning, A., Ott, M. (2017), Inductively heated magnetic nanoparticle-ansamitocin conjugates lead to decreased cell proliferation in vitro and attenuation of tumor growth in vivo. *Chem. Eur. J.*, ***23***, 12326–12337.

[24] Wang, L., Balakrishnan, A., Candito, D., Xie, Y., Seidel, K., Bigall, N., Ott, M., Kirschning, A. (2017), A bio-chemosynthetic approach to superparamagnetic iron oxide-ansamitocin conjugates for use in magnetic drug targeting (MDT). *Chem. Eur. J.*, ***23***, 2265–2270.

[25] Dudutienė, V., Zubrienė, A., Smirnov, A., Gylytė, J., Timm, D., Manakova, E., Matulis, D. (2013), 4-Substituted-2,3,5,6-tetrafluorobenzenesulfonamides as inhibitors of carbonic anhydrases I, II, VII, XII, and XIII. *Bioorg. Med. Chem.*, ***21***, 2093–2106.

[26] Dudutienė, V., Matulienė, J., Smirnov, A., Timm, D.D., Zubrienė, A., Baranauskienė, L., Morkūnaitė, V., Smirnovienė, J., Michailovienė, V., Juozapaitienė, V. and Mickevičiūtė, A. (2014), Discovery and characterization of novel selective inhibitors of carbonic anhydrase IX. *J. Med. Chem.*, ***57***, 9435–9446.

[27] Cazzamalli, S., Dal Corso, A., Neri, D. (2016), Acetazolamide Serves as Selective Delivery Vehicle for Dipeptide-Linked Drugs to Renal Cell Carcinoma. *Mol. Cancer Ther*., ***15***, 2926–2935.

[28] Krall, N., Pretto, F., Decurtins, W., Bernardes, G. J., Supuran, C. T., Neri, D. (2014), A small-molecule drug conjugate for the treatment of carbonic anhydrase IX expressing tumors. *Angew. Chem., Int. Ed.*, ***53***, 4231–4235.

[29] Breinin, G.M. and Gortz, H. (1954), Carbonic anhydrase inhibitor acetazoleamide (Diamox): A new approach to the therapy of glaucoma. *AMA Arch. Ophthalmol.*, ***52***, 333–348.

[30] Supuran, C. T. (2011), Carbonic anhydrase inhibitors and activators for novel therapeutic applications. *Future Med. Chem.*, ***3***, 1165–1180.

[31] Alterio, V., Di Fiore, A., D'Ambrosio, K., Supuran, C. T., & De Simone, G. (2012), Multiple binding modes of inhibitors to carbonic anhydrases: how to design specific drugs targeting 15 different isoforms? *Chem. Rev.*, ***112***, 4421–4468.

[32] Krishnamurthy, V. M., Bohall, B. R., Kim, C. Y., Moustakas, D. T., Christianson, D. W., Whitesides, G. M. (2007), Thermodynamic parameters for the association of fluorinated benzenesulfonamides with bovine carbonic anhydrase II. *Chem. Asian J.*, ***2***, 94–105.

[33] Krishnamurthy, V. M., Kaufman, G. K., Urbach, A. R., Gitlin, I., Gudiksen, K. L., Weibel, D. B., Whitesides, G. M. (2008), Carbonic anhydrase as a model for biophysical and physical-organic studies of proteins and protein ligand binding. *Chem. Rev.*, ***108***, 946–1051.